Kobe University Repository : Kernel

PDF issue: 2026-11-22

Dynamic J integral, separated dynamic J integral and component separation method for dynamic interfacial fracture mechanics in piezoelectric bimaterials

Nishioka, Toshihisa
Shen, Shengping
Yu, Jiahuan

(Citation)
International Journal of Fracture,122(3-4):101-130

(Issue Date)
2003-08

(Resource Type)
journal article

(Version)
Accepted Manuscript

(URL)
https://hdl.handle.net/20.500.14094/90000036

KOBE UNIVERSITY

R401

02.12.8

Dynamic *J* integral, Separated Dynamic *J* integrals and Component Separation Method for Dynamic Interfacial Fracture Mechanics for Piezoelectric Bimaterials

Contents

Abstract 1

1. Introduction 2

2. Governing equations and boundary conditions in a piezoelectric material under dynamic conditions . 4

3. The near-tip stress and electric displacement fields for a dynamically propagating interfacial crack in a piezoelectric material 5

4. Dynamic *J* integral for piezoelectric materials 9

4.1 Path independent dynamic *J* integral for elastic materials 9

4.2 Path independent dynamic *J* integral for piezoelectric materials 11

4.3 Relationships between the dynamic *J* integral and the stress and electric displacement intensity factors 14

5. Separated dynamic *J* integral for interfacial cracks in nonhomogeneous piezoelectric materials 15

6. Component separation method 16

6.1 Basic equations for transverse piezoelectric materials 17

6.2 Anti-plane deformation and in-plane electric potential 18

6.3 In-plane deformation and in-plane electric potential 19

6.3.1 Case of imaginary oscillatory singularity 20

6.3.2 Case of real oscillatory singularity 22

7. Numerical examples 24

8. Conclusions 28

References 29

Dynamic *J* integral, Separated Dynamic *J* integrals and Component Separation Method for Dynamic Interfacial Fracture Mechanics for Piezoelectric Bimaterials

Toshihisa Nishioka*, Shengping Shen and Jiahuan Yu

Simulation Engineering Laboratory

Department of Ocean Mechanical Engineering

Kobe University of Mercantile Marine

5-1-1 Fukae Minamimachi, Higashinada-ku, Kobe 658-0022, Japan

Abstract

First, the near-tip stress and electric displacement fields are analytically solved for a dynamically propagating interfacial crack in a piezoelectric bimaterial. Second, from the rate formulation of the energy balance in a piezoelectric material, the path independent dynamic *J* integral is derived, which has the physical significance of the energy release rate. Using the present near-tip analytical solutions, the relationships between the dynamic *J* integral and the stress and electric displacement intensity factors are also obtained. It is shown that the path independent dynamic *J* integral contains the static *J* integral and the dynamic *J* integral for elastic materials, and static *J* integral for piezoelectric materials as special cases. Third, for an interfacial crack in a piezoelectric bimaterial, the path independent separated dynamic *J* integrals are derived, which have the physical significance of energy flow rates into the propagating interfacial crack tip from the individual material sides or, equivalently, the separated dynamic energy release rates. Fourth, to accurately evaluate mixed-mode stress and electric displacement intensity factors, the component separation method of the dynamic *J* integral is developed. Finally, the finite element analyses of a static stationary interfacial crack in a piezoelectric bimaterial subject to mechanical, electrical and combined loading are carried out to demonstrate the applicability of the generalized (dynamic) *J* integral and the separated *J* integral, and the component separation method.

KEYWORDS:

Piezoelectric Material, Interfacial Crack, Dynamic J Integral, Energy Release Rate, Separated Dynamic J Integrals, Component Separation Method, Stress Intensity Factor, Electric Displacement Intensity Factor

*Corresponding author. Tel./ fax: +81-78-431-6282

E-mail address: nishioka@cc.kshosen.ac.jp (T. Nishioka)

---

1. Introduction

Nowadays, piezoelectric materials are used in sophisticated areas such as aerospace, mechanical and electronic technologies due to their important mechanical reliability. Cracks and delaminations which are initial typical damage phenomena in piezoelectric solids, may result in significant changes of the static and dynamic response of the structure. The mathematical descriptions of elastic fields induced by defects such as cracks, inclusions in piezoelectric solids are hard to obtain because of two factors that are difficult to determine: electro-elastic coupling effects and material anisotropy.

Although, real piezoelectric materials behave nonlinearly, in particular, under high level of mixed applied electric or mechanical loadings, a linear electro-elastic analysis is the first step to understand the fracture behavior of piezoelectric materials. It is extremely important to understand the fracture and damage processes and to develop theoretical foundations of fracture mechanics and numerical tools which are able to predict the fracture and damage in smart materials and structures.

Most of the analyses of cracked piezoelectric bodies that have been done are quasi-static (Kuo and Barnett 1991, Suo, Barnett and Wills 1992, Shen and Kuang 1998). Dascalu and Maugin (1995) investigated steady-state crack propagation in piezoelectric materials. For elastodynamic fracture

mechanics, Nishioka and Atluri (1983) first derived the path-independent dynamic J integral, which has the physical significance of dynamic energy release rate (Freund 1972). Furthermore, for dynamic interfacial fracture mechanics, Nishioka and Yasin (1999) have developed the separated dynamic J integrals, which are equivalent to the separated energy release rates from individual material sides. Recently, in order to accurately evaluate mixed-mode stress intensity factors, the component separation method (Nishioka, Murakami and Takemoto 1990) has been extended to static and dynamic interfacial crack problems (Nishioka, Syano and Fujimoto 2000, Nishioka, Hu and Fujimoto 2002). We aim here to extend the dynamic J integral, the separated dynamic J integral and the component separation method to dynamic interfacial fracture mechanics for piezoelectric materials.

The structure and contents of this paper are arranged as follows. In section 2, the governing equations and boundary conditions in a piezoelectric material under dynamic conditions are presented fully for case of reference. In section 3, to investigate the crack-tip asymptotic field, the near-tip stress and electric displacement fields for a dynamically propagating interfacial crack in a piezoelectric material are analytically solved and expressed in term of complex vector.

The path independent dynamic J integral concept of pure elastic case proposed by Nishioka and Atluri (1983) is extended to homogeneous piezoelectric materials in section 4. Furthermore, using the presently obtained near-tip analytical solutions, the relationships between the dynamic J integral and the stress and electric displacement intensity factors are obtained. In section 5, for piezoelectric bimaterials the path independent separated dynamic J integrals that have the physical significance of energy flow rates into an interfacial crack tip from the adjacent individual material sides are presented. In section 6, to accurately evaluate mixed-mode stress and electric displacement intensity factors, the component separation method of the dynamic J integral is developed.

Finally in section 7, the finite element analyses of a static stationary interfacial crack in the piezoelectric bimaterial of PZT-4 and PZT-5H subject to mechanical, electrical and combined loadings are carried out to demonstrate the applicability of the path independent dynamic J integral,

the separated J integral and the component separation method.

2. Governing equations and boundary conditions in a piezoelectric material under dynamic conditions

We use the mechanical displacement vector u_i and the scalar electric potential ϕ as the primary field variables in piezoelectric materials. Then, the mechanical strain tensor ε_{ij} and the electric field vector E_i can be deduced from these primary field variables by gradient operations:

$$\varepsilon_{ij} = \frac{1}{2}(u_{i,j} + u_{j,i}), \quad E_i = -\phi_{,i}, \tag{1}$$

where $(\,)_{,i}$ indicates the partial derivative of $(\,)$ with respect to the coordinate X_i.

Using these quantities, the electric enthalpy density in linear piezoelectric materials is expressed as (Tiersten 1969):

$$H(\varepsilon_{ij}, E_i) = \frac{1}{2}C_{ijkl}\,\varepsilon_{ij}\,\varepsilon_{kl} - \frac{1}{2}\kappa_{ij}E_iE_j - e_{ikl}\,\varepsilon_{kl}E_i, \tag{2}$$

where C_{ijkl} κ_{ik} and e_{ikl} are the elastic constants, the dielectric constants and piezoelectric constants, respectively. The repeated indices imply summation. The constitutive equation for the anisotropic piezoelectric material can be written as (Pak 1990):

$$\sigma_{ij} = \frac{\partial H}{\partial \varepsilon_{ij}} = C_{ijkl}\,\varepsilon_{kl} - e_{kij}E_k \tag{3}$$

$$D_i = \frac{\partial H}{\partial \phi_{,i}} = -\frac{\partial H}{\partial E_i} = e_{ikl}\,\varepsilon_{kl} + \kappa_{ik}E_k, \tag{4}$$

where σ_{ij} is the mechanical stress tensor, and D_i is the electric displacement vector. Substituting Eqs. (2) and (3) into Eq. (1), the electric enthalpy density can be rewritten by

$$H(\varepsilon_{ij}, E_i) = \frac{1}{2}\sigma_{ij}\,\varepsilon_{ij} - \frac{1}{2}D_iE_i = \frac{1}{2}\sigma_{ij}\,\varepsilon_{ij} + \frac{1}{2}D_i\phi_{,i}. \tag{5}$$

The following symmetry conditions hold (Suo, Barnett and Wills 1992):

$$C_{ijkl} = C_{lkji} = C_{jikl} = C_{ijlk}, \quad \kappa_{ij} = \kappa_{ji}, \quad e_{ikl} = e_{ilk}. \tag{6}$$

Taking account of the inertial effect, the linear and momentum equilibrium equations and the electrical balance equation can be expressed as

$$\sigma_{ij,j} + \bar{f}_i = \rho \ddot{u}_i \tag{7}$$

$$\sigma_{ij} = \sigma_{ji} \tag{8}$$

$$D_{i,i} + \overline{Q} = 0, \tag{9}$$

where $\bar{f}_i$ is a body force vector per unit volume, and the upper bar denotes an applied quantity. ρ is the mass density. $\ddot{u}_i$ is the acceleration of the material point. $\overline{Q}$ is applied body charge per unit volume.

The mechanical and geometrical boundary conditions are

$$t_i \equiv \sigma_{ij} n_j = \bar{t}_i \text{ on } S_t \tag{10}$$

$$u_i = \overline{u_i} \text{ on } S_u, \tag{11}$$

where t_i is a traction force vector per unit area. n_j is the unit normal vector. Furthermore, the electric boundary conditions are

$$q \equiv n_i D_i = \overline{q} \text{ on } S_q \tag{12}$$

$$\phi = \overline{\phi} \text{ on } S_\phi, \tag{13}$$

where q is the electric flux. $\overline{q}$ and $\overline{\phi}$ are applied surface charge and potential per unit surface area.

3. The near-tip stress and electric displacement fields for a dynamically propagating interfacial crack in a piezoelectric material

Figure 1 shows a planar interfacial crack in a piezoelectric material. Materials 1 and 2 occupy the two half-spaces. Consider a Cartesian coordinate (X_1, X_2, X_3) with its origin at the middle of the interfacial crack between two bonded dissimilar, anisotropic piezoelectric solids. The X_3-axis is in the out-of-plane direction. The X_1-axis is directed along the line of the crack and X_2-axis along the direction of the perpendicular bisector of the crack. The generalized two-dimensional deformation is considered in which the three components of displacement and the electric potential depend only on the in-plane coordinates.

In this section, for convenience, the subscripts (1) and (2) are used to designate the upper and

lower materials, which will be dropped unless it is necessary to distinguish the upper and lower half-spaces. Furthermore, without loss of generality, the body forces and the body charge are assumed to be zero ($\bar{f}_i = \overline{Q} = 0$).

Suppose that the crack is moving with a constant velocity C ($\equiv \frac{da}{dt}$) in the X_1 direction, where a is the crack length at time t. After sufficient time, a steady state will be attained. The displacements and stresses can be expressed in the form:

$$u_i = u_i(X_1 - Ct, X_2), \tag{14}$$

$$\sigma_{ij} = \sigma_{ij}(X_1 - Ct, X_2). \tag{15}$$

Substituting Eqs. (3) and (4) into Eqs. (7) and (9), respectively, the dynamic governing equations for piezoelectric materials are obtained as (Nishioka and Shen 2001):

$$\left(C_{ijrs}\, u_r + e_{sji}\, \phi\right)_{,si} = \rho \frac{\partial^2 u_j}{\partial t^2} \tag{16}$$

$$\left(-\kappa_{is}\, \phi + e_{irs}\, u_r\right)_{,si} = 0. \tag{17}$$

Denoting

$$\mathbf{U} = \left[u_1 \;\; u_2 \;\; u_3 \;\; \phi\right]^T, \;\; \mathbf{t} = \left[\sigma_{21} \;\sigma_{22} \;\sigma_{23} \;D_2\right]^T \text{ and } \;\; \mathbf{s} = \left[\sigma_{11} \;\sigma_{12} \;\sigma_{13} \;D_1\right]^T, \tag{18}$$

Equations (16) and (17) can be rewritten as

$$\mathbf{Q}_1 \mathbf{U}_{,11}(X_1, X_2, t) + \left(\mathbf{R} + \mathbf{R}^T\right)\mathbf{U}_{,12}(X_1, X_2, t) + \mathbf{W}\mathbf{U}_{,22}(X_1, X_2, t) = \rho \frac{\partial^2 \mathbf{U}(X_1, X_2, t)}{\partial t^2}, \tag{19}$$

where

$$\mathbf{Q}_1 = \begin{bmatrix} \mathbf{Q}_0 & \mathbf{e}_{11} \\ \mathbf{e}_{11}^T & -\varepsilon_{11} \end{bmatrix}, \mathbf{R} = \begin{bmatrix} \mathbf{R}_0 & \mathbf{e}_{21} \\ \mathbf{e}_{12}^T & -\varepsilon_{12} \end{bmatrix}, \mathbf{W} = \begin{bmatrix} \mathbf{W}_0 & \mathbf{e}_{22} \\ \mathbf{e}_{22}^T & -\varepsilon_{22} \end{bmatrix} \tag{20}$$

with

$$\left(\mathbf{Q}_0\right)_{ik} = C_{i1k1}, \left(\mathbf{R}_0\right)_{ik} = C_{i1k2}, \left(\mathbf{W}_0\right)_{ik} = C_{i2k2} \;\; (i,k=1,2,3), \;\; \mathbf{e}_{ik} = \left[e_{i1k}\, e_{i2k}\, e_{i3k}\right]^T, \;\; (i,k=1,2). \tag{21}$$

From the constitutive relations, we have

$$\mathbf{t} = \mathbf{R}^T \mathbf{U}_{,1} + \mathbf{W}\mathbf{U}_{,2} \quad \mathbf{s} = \mathbf{Q}_1 \mathbf{U}_{,1} + \mathbf{R}\mathbf{U}_{,2}. \tag{22}$$

For convenience, we introduce $\mathbf{L} = diag[\,\rho \;\; \rho \;\; \rho \;\; 0\,]$. By introducing the moving coordinate

$(x_1^0, x_2^0)=(X_1 - Ct, X_2)$, Equation (19) reduces to

$$\mathbf{Q}\mathbf{U}_{,11}+(\mathbf{R}+\mathbf{R}^T)\mathbf{U}_{,12}+\mathbf{W}\mathbf{U}_{,22}=0, \tag{23}$$

where

$$\mathbf{Q}(C)=\mathbf{Q}_1 - \rho C^2\mathbf{L}. \tag{24}$$

In general, the extended displacements and stresses can be represented as

$$\mathbf{u}=\mathbf{A}\mathbf{f}(z)+\overline{\mathbf{A}\mathbf{f}}(z) \tag{25}$$

$$\mathbf{t}=\mathbf{B}\mathbf{f}'(z)+\overline{\mathbf{B}\mathbf{f}'}(z), \tag{26}$$

where $\mathbf{A}=[\mathbf{a}_1\ \mathbf{a}_2\ \mathbf{a}_3\ \mathbf{a}_4]$, $\mathbf{B}=[\mathbf{b}_1\ \mathbf{b}_2\ \mathbf{b}_3\ \mathbf{b}_4]$. In above, $z_\alpha=x_1^0+p_\alpha x_2^0$. $\mathbf{a}_\alpha$ and p_α are determined by the following eigen equations (Shen and Kuang 1998):

$$\mathbf{J}(p)\mathbf{a}=\left[\mathbf{Q}+(\mathbf{R}+\mathbf{R}^T)p+\mathbf{W}p^2\right]\mathbf{a}=0. \tag{27}$$

To determine the eigenvalues p_α, from Eq. (27) we have

$$\left|(\mathbf{Q}_1 - \rho C^2\mathbf{I})+(\mathbf{R}+\mathbf{R}^T)p+\mathbf{W}p^2\right|=0. \tag{28}$$

Equation (28) has eight roots which cannot be real. The eight roots form four conjugate pairs and we shall choose $\mathbf{Im}(p_\alpha)>0$ for $\alpha=1,2,3,4$. The matrix $\mathbf{A}$ and $\mathbf{B}$ have the following correlation

$$b_\alpha=(\mathbf{R}^T+p_\alpha\mathbf{W})\mathbf{a}_\alpha=-\frac{1}{p_\alpha}(\mathbf{Q}+p_\alpha\mathbf{R})\mathbf{a}_\alpha. \tag{29}$$

The matrix $\mathbf{Y}=i\mathbf{A}\mathbf{B}^{-1}$, is a Hermitian matrix, and for interfacial crack, we define a matrix

$$\mathbf{H}=\mathbf{Y}_{(1)}+\overline{\mathbf{Y}}_{(2)}, \tag{30}$$

which is also Hermitian.

Let ε, κ and $\mathbf{\Lambda}$ be the eigenvalues and eigenvectors of the following equation, respectively:

$$(\overline{\mathbf{H}}-e^{2\pi\varepsilon}\mathbf{H})\mathbf{\Lambda}=0. \tag{31}$$

The matrix $\mathbf{H}$ can also be expressed by $\mathbf{H}=\mathbf{V}+i\mathbf{F}$, where $\mathbf{V}$ is real and symmetric and $\mathbf{F}$ is real and antisymmetric, and $\mathbf{E}=\mathbf{F}\mathbf{V}^{-1}$. Then the results can therefore be expressed as

$$\varepsilon=\frac{1}{\pi}\tanh^{-1}\omega_1 \text{ and } \kappa=\frac{1}{\pi}\tan^{-1}\omega_2 \tag{32}$$

$$\omega_1=\left[(b^2-c)^{1/2}-b\right]^{1/2},\ \omega_2=\left[(b^2-c)^{1/2}+b\right]^{1/2},\ b=\frac{1}{4}tr[\mathbf{E}^2] \text{ and } c=|\mathbf{E}|, \tag{33}$$

where ε, κ are the oscillatory indices.

We also introduce the following expression:

$$\mathbf{\Lambda} diag[\mu_\alpha]\mathbf{\Lambda}^{-1}=\mathbf{G}_1\mu_1+\overline{\mathbf{G}}_1\mu_2+\mathbf{G}_3\mu_3+\mathbf{G}_4\mu_4, \tag{34}$$

where μ_α are arbitrary functions of z, and

$$\mathbf{G}_1=\frac{1}{2(\omega_1^2+\omega_2^2)}\left\{\left[\omega_2^2\mathbf{I}-\mathbf{E}^2\right]+i\omega_1^{-1}\left[\omega_2^2\mathbf{I}-\mathbf{E}^2\right]\mathbf{E}\right\} \tag{35.a}$$

$$\mathbf{G}_3=\frac{1}{2(\omega_1^2+\omega_2^2)}\left\{\left[\omega_1^2\mathbf{I}+\mathbf{E}^2\right]-\omega_2^{-1}\left[\omega_1^2\mathbf{I}+\mathbf{E}^2\right]\mathbf{E}\right\} \tag{35.b}$$

$$\mathbf{G}_4=\frac{1}{2(\omega_1^2+\omega_2^2)}\left\{\left[\omega_1^2\mathbf{I}+\mathbf{E}^2\right]+\omega_2^{-1}\left[\omega_1^2\mathbf{I}+\mathbf{E}^2\right]\mathbf{E}\right\}. \tag{35.c}$$

This expression is very useful in computation, because it avoids solving the eigen equation (31).

For this problem, the stress and electric displacement intensity factors can be expressed in the form for static case (Shen and Kuang 1998) as

$$\mathbf{K}\equiv\left[K_1\ K_2\ K_3\ K_4\right]^T=\lim_{r\to 0}\sqrt{2\pi r}\,\mathbf{\Lambda} diag\left[r^{-i\varepsilon}\ r^{i\varepsilon}\ r^{-\kappa}\ r^{\kappa}\right]\mathbf{\Lambda}^{-1}\left[\sigma_{12}\ \sigma_{22}\ \sigma_{23}\ D_2\right]^T, \tag{36}$$

where r stands for the distance from the crack tip, ε and κ involve the bimaterial constant and crack velocity, $\mathbf{\Lambda}$ is the eigenvector matrix associated with the eigenvalue problem in the Stroh formalism (see Eq. (34)). The above definition is identical with the convention (Hwu 1993, Beom and Atluri 1996), and provides a unique characterization of the crack tip. Due to the oscillatory singularity in the near-tip field, the individual stress and electric displacement intensity factors K_1, K_2, K_3 and K_4 for the interfacial crack cannot be uniquely associated with mode I, mode II, mode III and mode IV fracture as defined in homogeneous piezoelectric materials. However, K_1, K_2, K_3 and K_4 still represent four different modes of fracture behavior.

For the interfacial crack,

$$\mathbf{f}'_{(1)}(z)=\frac{1}{\sqrt{2\pi z}}\mathbf{B}_{(1)}^{-1}\mathbf{\Lambda} diag\left[z^{i\varepsilon}\ z^{-i\varepsilon}\ z^{\kappa}\ z^{-\kappa}\right]\mathbf{\Lambda}^{-1}\left(\mathbf{I}+\overline{\mathbf{H}}^{-1}\mathbf{H}\right)^{-1}\mathbf{K} \tag{37.a}$$

$$\bar{\mathbf{f}}_{(2)}(z)=\frac{1}{\sqrt{2\pi z}}\mathbf{B}_{(2)}^{-1}\mathbf{\Lambda} diag\left[z^{i\varepsilon}\ z^{-i\varepsilon}\ z^{\kappa}\ z^{-\kappa}\right]\mathbf{\Lambda}^{-1}\left(\mathbf{I}+\overline{\mathbf{H}}^{-1}\mathbf{H}\right)^{-1}\mathbf{K} \tag{37.b}$$

in the upper half-space, and

$$\bar{\mathbf{f}}'_{(1)}(z)=\frac{1}{\sqrt{2\pi z}}\mathbf{B}_{(1)}^{-1}\overline{\mathbf{H}}^{-1}\mathbf{H}\mathbf{\Lambda} diag\left[z^{i\varepsilon}\ z^{-i\varepsilon}\ z^{\kappa}\ z^{-\kappa}\right]\mathbf{\Lambda}^{-1}\left(\mathbf{I}+\overline{\mathbf{H}}^{-1}\mathbf{H}\right)^{-1}\mathbf{K} \tag{38.a}$$

$$f_{(2)}(z)=\frac{1}{\sqrt{2\pi z}}\mathbf{B}_{(2)}^{-1}\overline{\mathbf{H}}^{-1}\mathbf{H}\Lambda diag[\,z^{i\varepsilon}\ z^{-i\varepsilon}\ z^{\kappa}\ z^{-\kappa}\,]\Lambda^{-1}(\mathbf{I}+\overline{\mathbf{H}}^{-1}\mathbf{H})^{-1}\mathbf{K} \tag{38.b}$$

in the lower half-space.

The crack opening displacements and electric potential jump at distance r behind the crack tip can be obtained from Eq. (25) and expressed as

$$[\,\delta_1\ \delta_2\ \delta_3\ \delta_4\,]^T$$

$$=\frac{4\sqrt{r}}{\sqrt{2\pi}}\mathbf{H}\Lambda diag\left[\ r^{i\varepsilon}\frac{\cosh\pi\varepsilon}{1+2i\varepsilon}\quad r^{-i\varepsilon}\frac{\cosh\pi\varepsilon}{1-2i\varepsilon}\quad r^{\kappa}\frac{\cos\pi\kappa}{1+2\kappa}\quad r^{-\kappa}\frac{\cos\pi\kappa}{1-2\kappa}\ \right]\Lambda^{-1}(\mathbf{I}+\overline{\mathbf{H}}^{-1}\mathbf{H})^{-1}[\,K_1\ K_2\ K_3\ K_4\,]^T. \tag{39}$$

The influences of material properties and crack velocity on the near-tip fields for interfacial crack are reflected through the oscillation indices ε and κ, and the Hermitian matrix $\mathbf{H}$, to which the eigenvector matrix $\mathbf{\Lambda}$ is related.

4. Dynamic J integral for piezoelectric materials

4.1 Path independent dynamic J integral for elastic materials

The static J integral (Rice 1968) has played an important role in static fracture mechanics. From the theoretical and computational points of view, the static J integral has the following salient features: (i) it physically represents the energy release rate; (ii) it has the property of the path-independent integral, which gives a unique value for an arbitrary integral path surrounding the crack tip; (iii) it can be related to the stress intensity factors by arbitrarily shrinking the integral path to the crack tip.

In the case of elastodynamic fracture mechanics, Nishioka and Atluri (1983) have derived the dynamic J integral (J') which has the aforementioned three features. For a dynamically propagating crack or a stationary crack under dynamic loading in an elastic solid as shown in Fig. 2, the global-axis components of the dynamic J integral can be expressed by

$$J'_k=\lim_{\Gamma_\varepsilon\to 0}\int_{\Gamma_\varepsilon}\left[(W+T)n_k-t_i u_{i,k}\right]dS \tag{40.a}$$

$$= \lim_{\Gamma_\varepsilon \to 0} \int_{\Gamma+\Gamma_c} \left[(W+T)n_k - t_i u_{i,k}\right] dS + \int_{V_\Gamma - V_\varepsilon} \left[(\rho \ddot{u}_i - \bar{f}_i) u_{i,k} - \rho \dot{u}_i \dot{u}_{i,k}\right] dV \tag{40.b}$$

where Γ_ε is the near field integral path (see Fig. 2), while Γ and Γ_c are the far field path and the crack face integral path, respectively. Γ connects any two points on opposite sides of the crack surface and enclosing the crack tip. Physically, the near-tip region V_ε can be considered as the process zone in which micro-processes associated with fracture occur. W and T are the strain and kinetic energy densities, respectively, and given by

$$W = \frac{1}{2}\sigma_{ij}\varepsilon_{ij} \text{ and } T = \frac{1}{2}\rho \dot{u}_i \dot{u}_i. \tag{41.a, b}$$

The crack-axis components of the dynamic J integral can be expressed by the following coordinate transformation:

$$J_l^0 = \alpha_{lk} J_k. \tag{42}$$

where α_{lk} is the coordinate transformation tensor. Using a circular near-field path that shrinks to the propagating crack tip, the dynamic J integral can be related to the instantaneous stress intensity factors for the elastodynamically propagating crack with velocity C, as in (Nishioka and Atluri 1983):

$$J_1^0 = \frac{1}{2\mu}\left\{A_I(C)K_I^2 + A_{II}(C)K_{II}^2 + A_{III}(C)K_{III}^2\right\} \text{ and } J_2^0 = -\frac{A_{IV}(C)}{\mu}K_I K_{II}, \tag{43.a, b}$$

where $A_M(C)$ $(M=I, II, III, IV)$ are functions of crack velocity C and given in (Nishioka and Atluri 1983). For a stationary crack $(C=0)$ under impact as well as static conditions, the velocity functions reduce to $A_I(0) = A_{II}(0) = (\kappa+1)/4$, $A_{III}(0) = 1$, and $A_{IV}(0)=(\kappa+1)/4$. Then the dynamic energy release rate G can be expressed by

$$G = J_1^0 = J_1 \cos\theta_0 + J_2 \sin\theta_0. \tag{44}$$

In most numerical analyses, far-field integrals are usually used to evaluate the values of the dynamic J integral. In this case, it is convenient to consider the following expression taking the limit of $V_\varepsilon \to 0$ $(\Gamma_\varepsilon \to 0)$:

$$J_k = \int_{\Gamma+\Gamma_c} \left[(W+K)n_k - t_i u_{i,k}\right] dS + \int_{V_\Gamma} \left[(\rho\ddot{u}_i - \bar{f}_i)u_{i,k} - \rho\dot{u}_i\dot{u}_{i,k}\right] dV. \tag{45}$$

4.2 Path independent dynamic *J* integral for piezoelectric materials

We consider a dynamically propagating crack with the velocity of C in a linear piezoelectric material as shown in Fig. 3. The near field V_ε can be considered as an infinitesimal process zone near the propagating crack tip. Then, in consideration of global energy balance, the energy flux Φ into the process zone or the propagating crack tip per unit time can be expressed by

$$\Phi = G\cdot C = J_1^0 \cdot C = \frac{d\tilde{P}}{dt} - \frac{d\tilde{H}}{dt} - \frac{d\tilde{T}}{dt} \tag{46.a}$$

$$= \int_{\partial V} \left(t_i\dot{u}_i + q\dot{\phi}\right) dS + \int_V \left(\bar{f}_i\dot{u}_i + \bar{Q}\dot{\phi}\right) dV - \frac{d}{dt}\int_V (H+T)\, dV, \tag{46.b}$$

where $\tilde{P}$, $\tilde{H}$ and $\tilde{T}$ are the total input energy, the total electric enthalpy and the total kinetic energy. ∂V denotes the boundary of the volume V, and can generally be expressed by

$$\partial V = S_t + S_u = S_q + S_\phi. \tag{47}$$

For the volume $(V - V_\varepsilon)$ excluding the crack tip, the following energy balance holds:

$$\int_{\partial V - \Gamma_\varepsilon} \left(t_i\dot{u}_i + q\dot{\phi}\right) dS + \int_{V - V_\varepsilon} \left(\bar{f}_i\dot{u}_i + \bar{Q}\dot{\phi}\right) dV - \frac{d}{dt}\int_{V - V_\varepsilon} (H+T)\, dV = 0. \tag{48}$$

Substitution of Eq. (48) into Eq. (46) leads to the following expression for Φ:

$$\Phi = G\cdot C = J_1^0 \cdot C = \lim_{\Gamma_\varepsilon \to 0}\left\{\int_{\Gamma_\varepsilon} \left(t_i\dot{u}_i + q\dot{\phi}\right) dS + \int_{V_\varepsilon} \left(\bar{f}_i\dot{u}_i + \bar{Q}\dot{\phi}\right) dV - \frac{d}{dt}\int_{V_\varepsilon} (H+T)\, dV\right\}. \tag{49}$$

Introducing the moving coordinate system attached at the propagating crack tip (see Fig. 3), The rate of change in a quantity ( ) can be expressed by

$$\frac{d(\,)}{dt} \equiv \dot{(\,)} = \frac{\partial(\,)}{\partial t} - C\frac{\partial(\,)}{\partial x_1^0} = \frac{\partial(\,)}{\partial t} - C(\,)_{,1}. \tag{50}$$

Then, the first and second terms in the right hand side of Eq. (49) reduce to

$$\lim_{\Gamma_\varepsilon \to 0}\left\{\int_{\Gamma_\varepsilon}\left(t_i\dot{u}_i + q\dot{\phi}\right) dS + \int_{V_\varepsilon}\left(\bar{f}_i\dot{u}_i + \bar{Q}\dot{\phi}\right) dV\right\}$$

$$= \lim_{\Gamma_\varepsilon \to 0}\left\{\int_{\Gamma_\varepsilon}\left(t_i\frac{\partial u_i}{\partial t} + q\frac{\partial \phi}{\partial t}\right) dS + \int_{V_\varepsilon}\left(\bar{f}_i\frac{\partial u_i}{\partial t} + \bar{Q}\frac{\partial \phi}{\partial t}\right) dV - C\int_{\Gamma_\varepsilon}\left(t_i u_{i,1} + q\phi_{,1}\right) dS - C\int_{V_\varepsilon}\left(\bar{f}_i u_{i,1} + \bar{Q}\phi_{,1}\right) dV\right\} \quad (51.a)$$

$$= -C\lim_{\Gamma_\varepsilon \to 0}\left\{\int_{\Gamma_\varepsilon}\left(t_i u_{i,1} + q\phi_{,1}\right) dS\right\}. \quad (51.b)$$

In Eq. (51.a), only the third integral in the right hand side remains finite because of the singularities in the integrands, and all other integrals vanish after taking the limit of $\Gamma_\varepsilon \to 0$.

Furthermore, the third term in the right hand side of Eq. (49) reduces to

$$\lim_{\Gamma_\varepsilon \to 0}\left\{-\frac{d}{dt}\int_{V_\varepsilon}(H+T)\, dV\right\}$$

$$= -C\lim_{\Gamma_\varepsilon \to 0}\left\{\frac{d}{da}\int_{V_\varepsilon}(H+T)\, dV\right\} = -C\lim_{\Gamma_\varepsilon \to 0}\left\{-\int_{\Gamma_\varepsilon}(H+T)n_1\, dS + \int_{V_\varepsilon}\frac{\partial}{\partial a}(H+T)\, dV\right\} \quad (52.a)$$

$$= C\lim_{\Gamma_\varepsilon \to 0}\left\{\int_{\Gamma_\varepsilon}(H+T)n_1\, dS\right\}. \quad (52.b)$$

In Eq. (52.a), the concept of subtracting out singularity (Atluri, Nishioka and Nakagaki 1984) was utilized. The second integral in the right hand side of Eq. (52.a) also vanishes due to the weaker singularities of the integrands.

Substituting Eqs. (51.b) and (52.b) into Eq. (49), we obtain:

$$\Phi = G\cdot C = J_1^0\cdot C = C\lim_{\Gamma_\varepsilon \to 0}\left\{\int_{\Gamma_\varepsilon}\left[(H+T)n_1 - t_i u_{i,1} - q\phi_{,1}\right] dS\right\}. \quad (53)$$

Therefore, the dynamic energy release rate and the tangential crack-axis component of the dynamic J integral can be defined by

$$G = J_1^0 = \lim_{\Gamma_\varepsilon \to 0}\left\{\int_{\Gamma_\varepsilon}\left[(H+T)n_1 - t_i u_{i,1} - q\phi_{,1}\right] dS\right\}. \quad (54)$$

For numerical analyses, the use of the global coordinate system is generally more convenient

(see Fig. 2). Based on Eq. (54), the path independent dynamic J integral with respect to the global coordinate system can be derived as

$$J'_k = \lim_{\Gamma_\varepsilon \to 0} \int_{\Gamma_\varepsilon} \left[(H+T) n_k - t_i u_{i,k} - q \phi_{,k} \right] dS \tag{55.a}$$

$$= \lim_{\Gamma_\varepsilon \to 0} \int_{\Gamma+\Gamma_c} \left[(H+T) n_k - t_i u_{i,k} - q \phi_{,k} \right] dS + \int_{V_\Gamma - V_\varepsilon} \left[(\rho \ddot{u}_i - \bar{f}_i) u_{i,k} - \rho \dot{u}_i \dot{u}_{i,k} - \bar{Q} \phi_{,k} \right] dV . \tag{55.b}$$

Furthermore, for an infinitesimal process zone, the following expression is more convenient:

$$J'_k = \int_{\Gamma+\Gamma_c} \left[(H+T) n_k - t_i u_{i,k} - q \phi_{,k} \right] dS + \int_{V_\Gamma} \left[(\rho \ddot{u}_i - \bar{f}_i) u_{i,k} - \rho \dot{u}_i \dot{u}_{i,k} - \bar{Q} \phi_{,k} \right] dV \tag{56}$$

This expression is also very useful for numerical analyses.

The crack axis components of the dynamic J integral J'^0_k can be directly evaluated by using the crack-axis components of all quantities in Eqs. (55) and (56), or by using the same coordinate transformation as Eq. (42): i.e., $J'^0_l = \alpha_{lk} J'_k$.

The path independent dynamic J integral given by Eqs. (55) and (56) is valid for stationary cracks (C=0) under impact loading as well as for dynamically propagating cracks in piezoeletric materials. If we consider dynamic cracks in elastic materials without all electric effects, we have $H=W$, $q=0$, $\bar{Q}=0$. Then, the dynamic J integral for piezoelectric materials (see Eqs. (55) and (56)) coincides with the dynamic J integral for elastic materials derived by Nishioka and Atluri (1983) (see Eqs. (40) and (45)). Moreover, if both electrical and dynamic effects are ignored in Eqs. (55) and (56), the dynamic J integral for piezoeletric materials reduces to the static J integral derived by Rice (1968) and Budiansky and Rice (1973).

Furthermore, if we consider static cracks under static loading conditions in piezoelectric materials, the dynamic J integral with respect to the crack-axis coordinate system reduces to the static one:

$$J'^0_k = J^0_k = \int_{\Gamma+\Gamma_c} \left[H n_k - t_i u_{i,k} - q \phi_{,k} \right] dS - \int_{V_\Gamma} \left[\bar{f} u_{i,k} + \bar{Q} \phi_{,k} \right] dV . \tag{57}$$

The above expression coincides with the one derived by Kuna (1998). Moreover, if the body forces $\bar{f}_i$ and the body charge $\overline{Q}$ are ignored, the dynamic J integral J_1^0 coincides with the static J integral for piezoelectric materials derived by Cherepanov (1979) and Pak (1990):

Using the equivalent domain integral expression (Nikishkov and Atluri 1987, Moran and Shih 1987, Nishioka, Ichikawa and Maeda 1995), the dynamic J integral for piezoelectric materials can be rewritten as

$$J_k^0 = \int_{V_\Gamma} \left[(\sigma_{ij}u_{i,k} + D_j\phi_{,k})s_{,j} + (\rho\ddot{u}_i u_{i,k} - \rho\dot{u}_i\dot{u}_{i,k} - \bar{f}_i u_{i,k} - \overline{Q}\phi_{,k})s - (H + T)s_{,k}\right]dV, \tag{58}$$

where s is a continuous function, and takes $s=0$ on $\Gamma+\Gamma_c$ and $s=1$ at the crack tip.

4.3 Relationships between the dynamic J integral and the stress and electric displacement intensity factors

For a straight crack as shown in Fig. 1, $J_k^0 = J_k$. Using the near-tip stress and electric displacement fields derived in section 3 into Eq. (54), the dynamic J integral and the dynamic energy release rate can be related to the stress and electric displacement intensity factors. Following the detailed derivation described in Nishioka, Yu and Shen (2002), the dynamic J integrals can be written in the complex form for an anisotropic piezoelectric solid as

$$J_1^0 = \lim_{\varepsilon\to 0} \mathrm{Re}\left\{\sum_{k=1}^{4}\int_{\Gamma_\varepsilon} [f_k(z_k)]^2 dz_k\right\} = \frac{1}{2}\lim_{\varepsilon\to 0}\int_{\Gamma_\varepsilon}\left\{\mathbf{f}^T(z)\mathbf{f}(z) - \bar{\mathbf{f}}^T(z)\bar{\mathbf{f}}(z)\right\}dz, \tag{59}$$

where $f_k(z_k)$ are the analytic functions generating the singular part of the interfacial stress and electric displacement (see Eqs. (25) and (26)). In Eq. (59), a circular near-field path with radius of ε is used. A similar formulation was used by Wu (1991) for an interface crack in an anisotropic elastic bimaterial.

Noting that the eigenvectors satisfy the orthogonality relation (Suo, Barnett and Wills 1992),

$$\left(\mathbf{B}^{-1}\right)^T\mathbf{B}^{-1} = i\mathbf{Y} - i\bar{\mathbf{Y}}. \tag{60}$$

We can derive that

$$\mathbf{f'}_{(1)}^{T}(z)\mathbf{f'}_{(1)}(z) - \bar{\mathbf{f}}'_{(2)}{}^{T}(z)\bar{\mathbf{f}}'_{(2)}(z) = -\frac{i}{4\pi z}\mathbf{K}^{T}\mathbf{U}\mathbf{K}. \tag{61}$$

Then the dynamic J integral is evaluated with the near-tip fields as

$$J_1^0 = G = \frac{1}{4}\mathbf{K}^{T}\mathbf{U}\mathbf{K}, \tag{62}$$

where

$$\mathbf{U} = 2\left(\mathbf{H}^{-1} + \bar{\mathbf{H}}^{-1}\right)^{-1}. \tag{63}$$

It is noted that the above formulas are valid for both static and dynamic interfacial cracks.

For homogenous materials, these formulas can be simplified as

$$\left[\delta_1 \;\; \delta_2 \;\; \delta_3 \;\; \delta_4\right]^{T} = \frac{\sqrt{2r}}{\sqrt{\pi}}\mathbf{H}\left[K_1 K_2 K_3 K_4\right]^{T} \tag{64}$$

and

$$J_1^0 = G = \frac{1}{4}\mathbf{K}^{T}\mathbf{H}\mathbf{K}. \tag{65}$$

5. Separated dynamic J integral for interfacial cracks in nonhomogeneous piezoelectric materials

Recently Nishioka and Yasin (1999) derived the separated dynamic J integrals for an interfacial crack in an elastic bimaterial, which have the physical significance of energy flow rates into the propagating interfacial crack tip from the individual material sides or, equivalently, the separated dynamic energy release rates.

Considering a nonhomogeneous piezoelectric system with a dynamically propagating interfacial crack as shown in Fig. 4, we can extend the separated dynamic J integrals (Nishioka, and Yasin 1999) to piezoelectric materials as

$$J_k^{(m)} = \lim_{\Gamma_\varepsilon^{(m)}\to 0}\int_{\Gamma_\varepsilon^{(m)}}\left[(H+T)n_k - t_i u_{i,k} - q\phi_{,k}\right]ds \tag{66.a}$$

$$= \lim_{\Gamma_\varepsilon^{(m)}\to 0}\int_{\Gamma^{(m)}+\Gamma_C^{(m)}+\Gamma_l^{(m)}}\left[(H+T)n_k - t_i u_{i,k} - q\phi_{,k}\right]ds + \int_{V_\Gamma^{(m)}-V_\varepsilon^{(m)}}\left[(\rho\ddot{u}_i - \bar{f}_i)u_{i,k} - \rho\dot{u}_i\dot{u}_{i,k} - \bar{Q}\phi_{,k}\right]dV, \tag{66.b}$$

where m denotes the material number. $\Gamma_l^{(m)}$ $(m=1,2)$ are the integral paths along the interface in the

sides of the material 1 and 2, respectively. The integral paths are defined in Fig. 4. The path independence of the separated dynamic J integrals can be verified in a similar manner in Nishioka and Atluri (1983) and Nishioka and Yasin (1999). For numerical analyses the following expression is also convenient:

$$J_k^{(m)} = \int_{\Gamma^{(m)}+\Gamma_C^{(m)}+\Gamma_I^{(m)}} \left[(H+T)n_k - t_i u_{i,k} - q\phi_{,k} \right] ds + \int_{V_T^{(m)}} \left[(\rho\ddot{u}_i - \bar{f}_i)u_{i,k} - \rho\dot{u}_i\dot{u}_{i,k} - \overline{Q}\phi_{,k} \right] dV . \tag{67}$$

The crack axis components of the separated dynamic J integral can also be evaluated by the coordinate transformation:

$$J_l^{0(m)} = \alpha_{lk} J_k^{(m)} . \tag{68}$$

The separated dynamic J integrals also have the physical significance of the separated energy release rates $G^{(m)}$ which are the energy flow rates from material m $(m=1,2)$ into the propagating interfacial crack tip per unit crack extension. Thus, we have the following relations:

$$J_1^{0(m)} = G^{(m)} = J_1^{(m)} \cos\theta_0 + J_2^{(m)} \sin\theta_0 . \tag{69}$$

Furthermore, the dynamic J integral and the energy release rate can be obtained by the sum of the separated dynamic J integrals:

$$J_1^0 = J_1^{0(1)} + J_1^{0(2)} = G = G^{(1)} + G^{(2)} . \tag{70}$$

6. Component separation method

In order to accurately evaluate mixed-mode dynamic stress intensity factors, Nishioka, Murakami and Takemoto (1990) developed the component separation method of the dynamic J integral for various dynamic crack problems in homogeneous elastic materials. Furthermore, Nishioka, Syano and Fujimoto (2002) and Nishioka, Hu and Fujimoto (2002) also developed the component separation method for static and dynamic interfacial crack problems, respectively.

An alternative formulation to the component separation method was put forward by Yau and Wang (1984), who proposed the M_1 integral method for evaluating mixed-mode static stress intensity factors of an interfacial crack. In their method, the analytical solution for an appropriate

auxiliary problem is necessary. However, the auxiliary solution field is often difficult or impossible to construct even for static interface problems such as curved interfaces. In contrast, the component separation method does not require any fictitious auxiliary solution field, which represents a great advantage of the present method over the M_1 integral method.

In this paper, the component separation method is extended to piezoelectric materials.

6.1 Basic equations for transverse piezoelectric materials

In finite element analyses, the stress and electric displacement intensity factors obtained directly from the relationships with the near-tip displacements as given by Eq. (39) are not accurate. However, the ratios K_1/K_2, K_3/K_2 and K_4/K_2 can be calculated accurately in terms of crack surface displacement and electric potential ratios δ_1/δ_2, δ_3/δ_2 and δ_4/δ_2. Thus, the individual stress and electric displacement intensity factors K_1, K_2, K_3 and K_4 can be obtained from these ratios K_1/K_2, K_3/K_2 and K_4/K_2 in conjugation with the dynamic J integral or the energy release rate.

In this paper, we will consider a class of piezoelectric materials of practical significance that its constitutive equation has transverse symmetry around the poling axis (axis-2):

$$\begin{bmatrix}\sigma_{11}\\ \sigma_{22}\\ \sigma_{33}\\ \sigma_{23}\\ \sigma_{13}\\ \sigma_{12}\end{bmatrix}=\begin{bmatrix} c_{11} & c_{13} & c_{12} & 0 & 0 & 0\\ c_{13} & c_{33} & c_{13} & 0 & 0 & 0\\ c_{12} & c_{13} & c_{11} & 0 & 0 & 0\\ 0 & 0 & 0 & c_{44} & 0 & 0\\ 0 & 0 & 0 & 0 & (c_{11}-c_{12})/2 & 0\\ 0 & 0 & 0 & 0 & 0 & c_{44}\end{bmatrix}\begin{bmatrix}\varepsilon_{11}\\ \varepsilon_{22}\\ \varepsilon_{33}\\ 2\varepsilon_{23}\\ 2\varepsilon_{13}\\ 2\varepsilon_{12}\end{bmatrix}-\begin{bmatrix} 0 & e_{31} & 0\\ 0 & e_{33} & 0\\ 0 & e_{31} & 0\\ 0 & 0 & e_{15}\\ 0 & 0 & 0\\ e_{15} & 0 & 0\end{bmatrix}\begin{bmatrix}E_1\\ E_2\\ E_3\end{bmatrix} \tag{71}$$

$$\begin{bmatrix}D_1\\ D_2\\ D_3\end{bmatrix}=\begin{bmatrix} 0 & 0 & 0 & 0 & 0 & e_{15}\\ e_{31} & e_{33} & e_{31} & 0 & 0 & 0\\ 0 & 0 & 0 & e_{15} & 0 & 0\end{bmatrix}\begin{bmatrix}\varepsilon_{11}\\ \varepsilon_{22}\\ \varepsilon_{33}\\ 2\varepsilon_{23}\\ 2\varepsilon_{13}\\ 2\varepsilon_{12}\end{bmatrix}+\begin{bmatrix}\kappa_{11} & 0 & 0\\ 0 & \kappa_{33} & 0\\ 0 & 0 & \kappa_{11}\end{bmatrix}\begin{bmatrix}E_1\\ E_2\\ E_3\end{bmatrix}. \tag{72}$$

In the above equations, the elastic constant tensor and piezoelectric constant tensor are reduced to the matrix forms.

6.2 Anti-plane deformation and in-plane electric potential

At first, we consider the simplest case, the anti-plane deformation and in-plane electric potential for piezoelectric bimaterials. In this case, the crack front coincides with the poling axis and the x^0_1-x^0_3 plane coincides the isotropic plane. The in-plane displacements u_1 and u_3 are decoupled from the anti-plane displacement u_2 and the electric potential ϕ. We only consider the latter. For an interfacial crack, the in-plane displacements u_1 and u_3 contain an oscillatory singularity. However the field derived from the anti-plane displacement u_2 and the electric potential ϕ remains square root singular. In each material, the components of the crack tip field remain the same as the homogeneous one. For this case, we have

$$\mathbf{A}=\begin{bmatrix} 0 & 1 \\ 1 & e_{15}/\varepsilon_{11} \end{bmatrix}, \mathbf{B}=i\begin{bmatrix} e_{15} & \mu\alpha \\ -\varepsilon_{11} & 0 \end{bmatrix} \tag{73}$$

$$\mathbf{Y} = i\mathbf{A}\mathbf{B}^{-1} = \frac{\alpha^{-1}}{1+k}\begin{bmatrix} c_{44}^{-1} & ke_{15}^{-1} \\ ke_{15}^{-1} & l\varepsilon_{11}^{-1} \end{bmatrix}, k = \frac{e_{15}^2}{c_{44}\varepsilon_{11}}, \tag{74}$$

where

$$\alpha = \sqrt{1- C^2/C_s^2}, l = k - (1+k)\alpha \text{ and } C_s = \sqrt{\mu/\rho}, \ \mu = c_{44} + e_{15}^2/\varepsilon_{11}. \tag{75}$$

μ is the piezoelectrically stiffened elastic constant, C_s is the speed of the piezoelectrically stiffened bulk shear wave, C is the crack velocity, and ρ is the density of the material. As C=0, $\mathbf{Y}$ is reduced to the static value.

Now, the matrix $\mathbf{H}$ can be written as

$$\mathbf{H}=\mathbf{Y}_{(1)}+\overline{\mathbf{Y}}_{(2)}=\mathbf{Y}_{(1)}+\mathbf{Y}_{(2)}, \tag{76}$$

where the subscripts 1 and 2 represent the upper and lower material, respectively. The matrix $\mathbf{Y}_{(1)}$ and $\mathbf{Y}_{(2)}$ are given in Eq. (74) for each material.

By means of Eq. (62), the dynamic J integral and the energy release rate can be obtained as

$$J_1^0 = \frac{1}{4}\left[H_{11}K_2^2 + 2H_{12}K_2K_4 + H_{22}K_4^2\right], \tag{77}$$

where H_{11}, H_{12} and H_{22} are the elements of symmetric matrix $\mathbf{H}$, which can be expressed explicitly by means of Eqs. (73) and (74) as

$$H_{11}=\left(\frac{\alpha^{-1}c_{44}^{-1}}{1+k}\right)_{(1)}+\left(\frac{\alpha^{-1}c_{44}^{-1}}{1+k}\right)_{(2)},\quad H_{12}=H_{21}=\left(\frac{\alpha^{-1}ke_{15}^{-1}}{1+k}\right)_{(1)}+\left(\frac{\alpha^{-1}ke_{15}^{-1}}{1+k}\right)_{(2)},\quad H_{22}=\left(\frac{\alpha^{-1}l\varepsilon_{11}^{-1}}{1+k}\right)_{(1)}+\left(\frac{\alpha^{-1}l\varepsilon_{11}^{-1}}{1+k}\right)_{(2)}. \tag{78}$$

The crack opening displacement and electric potential jump at distance r behind the crack tip can be expressed as

$$\begin{bmatrix}\delta_2\\ \delta_4\end{bmatrix}=\sqrt{\frac{2r}{\pi}}\mathbf{H}\begin{bmatrix}K_2\\ K_4\end{bmatrix}. \tag{79}$$

Denoting $K=K_4/K_2$, $\delta=\delta_4/\delta_2$, then from Eq. (79), we obtain

$$K=\frac{n_4}{n_2} \tag{80}$$

with

$$n_2=H_{12}\delta-H_{22},\ n_4=H_{12}-H_{11}\delta. \tag{81}$$

Thus, combining Eqs. (79) and (77), one can get the stress intensity factor K_2 and the electric displacement intensity factor K_4 as

$$K_j=2n_j\mathbf{sgn}(\delta_2)\sqrt{\frac{J_1^0}{\left|H_{11}n_2^2+2H_{12}n_2n_4+H_{22}n_4^2\right|}},(j=2,4) \tag{82}$$

in which sgn( ) stands for the sign function.

6.3 In-plane deformation and in-plane electric potential

At first, we consider in-plane deformation and in-plane electric potential for homogenous piezoelectric materials. In this case, the crack plane perpendicular to the poling axis, and the anti-plane u_3 decouples from u_1, u_2, and ϕ. With u_3 ignored, the matrix $\mathbf{H}$ has the structure:

$$\mathbf{H}=\begin{bmatrix}H_{11} & 0 & 0\\ 0 & H_{22} & H_{23}\\ 0 & H_{23} & H_{33}\end{bmatrix}. \tag{83}$$

Here, $\mathbf{H}$ is real, and its elements H_{ij} should be computed numerically. It should be noted that here H_{11} and H_{22} are different from those in Eq. (78). Then we have the following equation for the crack opening displacement and electric potential jump at distance r behind the crack tip

$$[\delta_1\ \delta_2\ \delta_4]^T=\frac{\sqrt{2r}}{\sqrt{\pi}}\mathbf{H}[\mathbf{K}_1\mathbf{K}_2\mathbf{K}_4]^T. \tag{84}$$

Furthermore, the dynamic J integral and the energy release rate can be written as

$$J_1^0 = \frac{1}{4}\left[H_{11}K_1^2 + H_{22}K_2^2 + 2H_{23}K_2K_4 + H_{33}K_4^2\right]. \tag{85}$$

Denoting $q_1=\delta_1/\delta_2$, $q_2=\delta_4/\delta_2$ and

$$n_1=H_{22}H_{33}q_1-H_{23}^2q_1,\quad n_2=H_{11}H_{33}-H_{11}H_{23}q_2,\quad n_4=H_{11}H_{22}q_2-H_{11}H_{23}. \tag{86}$$

By appealing to Eqs. (84) and (85), we obtain

$$K_j = 2n_j\,\mathrm{sgn}(|\mathbf{H}|)\sqrt{\frac{J_1^0}{\left|H_{11}n_1^2+H_{22}n_2^2+2H_{23}n_2n_4+H_{33}n_4^2\right|}},\ (j=1,2,4) \tag{87}$$

with $|\mathbf{H}| = H_{11}(H_{22}H_{33} - H_{23}^2)$.

For interfacial cracks, we note that the matrix $\mathbf{H}$ takes the following forms

$$\mathbf{H}=\mathbf{V}+i\mathbf{F},\ \text{and}\ \mathbf{V}=\begin{bmatrix} v_{11} & 0 & 0 \\ 0 & v_{22} & v_{23} \\ 0 & v_{23} & v_{33} \end{bmatrix},\ \mathbf{F}=\begin{bmatrix} 0 & f_{12} & -f_{13} \\ -f_{12} & 0 & 0 \\ f_{13} & 0 & 0 \end{bmatrix}, \tag{88}$$

where v_{ij} and f_{ij} $(i,j=1,2,3)$ are the components of the matrices $\mathbf{V}$ and $\mathbf{F}$.

For homogeneous materials, $f_{12}=f_{13}=0$. For interfacial crack, the oscillatory singularity of the stress and electric field can be imaginary or real, which depends on whether $\mathrm{tr}[\mathbf{E}^2]$ is greater than 0, where $\mathbf{E}=\mathbf{F}\mathbf{V}^{-1}$ and tr[ ] stands for the trace of the matrix [ ]. We will discuss these two conditions, respectively.

6.3.1 Case of imaginary oscillatory singularity

When $\mathrm{tr}[\mathbf{E}^2]\le 0$, the oscillatory singularity is imaginary. In this condition, the crack opening displacement and electric potential jump at distance r behind the crack tip can be expressed as

$$\left[\delta_1\ \delta_2\ \delta_4\right]^T = \frac{4\sqrt{r}}{\sqrt{2\pi}}\mathbf{H}\mathbf{\Lambda}\,diag\left[r^{i\varepsilon}\frac{\cosh\pi\varepsilon}{1+2i\varepsilon}\quad r^{-i\varepsilon}\frac{\cosh\pi\varepsilon}{1-2i\varepsilon}\quad 1\right]\mathbf{\Lambda}^{-1}\left(\mathbf{I}+\overline{\mathbf{H}}^{-1}\mathbf{H}\right)^{-1}\left[K_1\ K_2\ K_4\right]^T. \tag{89}$$

To avoid solving the eigenvalue problem to determine the eigenvectors, we derive the following expression

$$\mathbf{\Lambda}\,diag\left[r^{i\varepsilon}\frac{\cosh\pi\varepsilon}{1+2i\varepsilon}\quad r^{-i\varepsilon}\frac{\cosh\pi\varepsilon}{1-2i\varepsilon}\quad 1\right]\mathbf{\Lambda}^{-1} = \mathbf{G}_1\xi_1 + \overline{\mathbf{G}}_1\overline{\xi}_1 + \mathbf{G}_3, \tag{90}$$

where

$$\xi_1 = r^{i\varepsilon}\frac{\cosh \pi\varepsilon}{1+2\,i\varepsilon} \tag{91}$$

$$\varepsilon = \frac{1}{2\pi}\ln\frac{1-\beta}{1+\beta},\ \beta = \sqrt{-\frac{1}{2}tr\left[\mathbf{E}^2\right]} = \left[-\frac{a_5 f_{12}+a_6 f_{13}}{\nu_{11}a_1}\right]^{\frac{1}{2}} \tag{92}$$

$$\mathbf{G}_1 = \frac{-1}{2\beta^2}\left[\mathbf{E}^2 - i\beta\mathbf{E}\right],\ \mathbf{G}_3 = \frac{1}{\beta^2}\left[\mathbf{E}^2 + \beta^2\mathbf{I}\right]. \tag{93}$$

Then the following relation can be proved

$$\mathbf{T}_1 = 2\mathbf{H}\left(\mathbf{I}+\overline{\mathbf{H}}^{-1}\mathbf{H}\right)^{-1} = 2\left(\overline{\mathbf{H}}^{-1}+\mathbf{H}^{-1}\right)^{-1} = \begin{bmatrix} \nu_{11}b_1 & 0 & 0 \\ 0 & a_2/\nu_{11} & a_3/\nu_{11} \\ 0 & a_3/\nu_{11} & a_4/\nu_{11} \end{bmatrix} = \mathbf{U} \tag{94}$$

$$\mathbf{T}_2 = \frac{2}{i}\mathbf{H}\mathbf{E}\left(\mathbf{I}+\overline{\mathbf{H}}^{-1}\mathbf{H}\right)^{-1} = \frac{2}{i}\left(\overline{\mathbf{H}}^{-1}+\mathbf{H}^{-1}\right)^{-1}\left(\overline{\mathbf{H}}^{-1}-\mathbf{H}^{-1}\right)\left(\overline{\mathbf{H}}^{-1}+\mathbf{H}^{-1}\right)^{-1} = \begin{bmatrix} 0 & -f_{12}b_1 & f_{13}b_1 \\ f_{12}b_1 & 0 & 0 \\ -f_{13}b_1 & 0 & 0 \end{bmatrix} \tag{95}$$

$$\mathbf{T}_3 = 2\mathbf{H}\mathbf{E}^2\left(\mathbf{I}+\overline{\mathbf{H}}^{-1}\mathbf{H}\right)^{-1} = -2\left(\overline{\mathbf{H}}^{-1}+\mathbf{H}^{-1}\right)^{-1}\left(\overline{\mathbf{H}}^{-1}-\mathbf{H}^{-1}\right)\left(\overline{\mathbf{H}}^{-1}+\mathbf{H}^{-1}\right)^{-1}\left(\overline{\mathbf{H}}^{-1}-\mathbf{H}^{-1}\right)\left(\overline{\mathbf{H}}^{-1}+\mathbf{H}^{-1}\right)^{-1}$$

$$= \begin{bmatrix} \frac{f_{12}a_5+f_{13}a_6}{a_1}b_1 & 0 & 0 \\ 0 & -\frac{f_{12}^2}{\nu_{11}}b_1 & \frac{f_{12}f_{13}}{\nu_{11}}b_1 \\ 0 & \frac{f_{12}f_{13}}{\nu_{11}}b_1 & -\frac{f_{13}^2}{\nu_{11}}b_1 \end{bmatrix} \tag{96}$$

with

$$a_1=\nu_{23}^2-\nu_{22}\nu_{33},\ a_2=\nu_{22}\nu_{11}-f_{12}^2,\ a_3=\nu_{23}\nu_{11}+f_{12}f_{13},\ a_4=\nu_{33}\nu_{11}-f_{13}^2,\ a_5=\nu_{33}f_{12}+\nu_{23}f_{13},\ a_6=\nu_{23}f_{12}+\nu_{22}f_{13},$$

$$b_0=\nu_{11}a_1+a_5f_{12}+f_{13}a_6,\ b_1=b_0/(\nu_{11}a_1). \tag{97}$$

Hence, Eq. (89) can be rewritten as

$$\left[\delta_1\ \ \delta_2\ \ \delta_4\right]^T = \frac{4\sqrt{r}}{\sqrt{2\pi}}\mathbf{H}\mathbf{\Lambda}diag\left[\ \xi_1\ \ \overline{\xi}_1\ \ 1\ \right]\mathbf{\Lambda}^{-1}\left(\mathbf{I}+\overline{\mathbf{H}}^{-1}\mathbf{H}\right)^{-1}\left[K_1\ K_2\ K_4\right]^T$$

$$= \sqrt{\frac{2r}{\pi}}\left\{\left[1-\mathbf{Re}\left(\xi_1\right)\right]\frac{1}{\beta^2}\mathbf{T}_3 - \mathbf{Im}\left(\xi_1\right)\frac{1}{\beta}\mathbf{T}_2 + \mathbf{T}_1\right\}\left[K_1\ K_2\ K_4\right]^T \tag{98}$$

or

$$\delta_1 = \sqrt{\frac{2r}{\pi}}\left\{\left[\left(1-\mathbf{Re}\,\xi_1\right)\frac{f_{12}a_5+f_{13}a_6}{\beta^2 a_1}+\nu_{11}\right]b_1K_1 + \mathbf{Im}\,\xi_1\frac{f_{12}b_1}{\beta}K_2 - \mathbf{Im}\,\xi_1\frac{f_{13}b_1}{\beta}K_4\right\}$$

$$\delta_2 = \sqrt{\frac{2r}{\pi}}\left\{-\mathbf{Im}\,\xi_1\frac{f_{12}b_1}{\beta}K_1 + \left[\frac{a_2}{\nu_{11}}-\left(1-\mathbf{Re}\,\xi_1\right)\frac{f_{12}^2b_1}{\beta^2\nu_{11}}\right]K_2 + \left[\frac{a_3}{\nu_{11}}+\left(1-\mathbf{Re}\,\xi_1\right)\frac{f_{12}f_{13}b_1}{\beta^2\nu_{11}}\right]K_4\right\}$$

$$\delta_4 = \sqrt{\frac{2r}{\pi}}\left\{ \mathrm{Im}\,\xi_1 \frac{f_{13}b_1}{\beta} K_1 + \left[\frac{a_3}{\nu_{11}} + \left(1 - \mathrm{Re}\,\xi_1\right)\frac{f_{12}f_{13}b_1}{\beta^2\nu_{11}} \right] K_2 + \left[\frac{a_4}{\nu_{11}} \left(1 - \mathrm{Re}\,\xi_1\right)\frac{f_{13}^2 b_1}{\beta^2\nu_{11}} \right] K_4 \right\}. \tag{99}$$

6.3.2 Case of real oscillatory singularity

When $\mathrm{tr}[\mathbf{E}^2]>0$, the oscillatory singularity is real. In this condition, the crack opening displacement and electric potential jump at distance r behind the crack tip can be expressed as

$$[\delta_1 \;\; \delta_2 \;\; \delta_4]^T = \frac{4\sqrt{r}}{\sqrt{2\pi}} \mathbf{H}\boldsymbol{\Lambda}\, diag\left[r^{\kappa}\frac{\cos\pi\kappa}{1+2\kappa} \;\; r^{-\kappa}\frac{\cos\pi\kappa}{1-2\kappa} \;\; 1 \right] \boldsymbol{\Lambda}^{-1}\left(\mathbf{I}+\bar{\mathbf{H}}^{-1}\mathbf{H}\right)^{-1}[K_1 \; K_2 \; K_4]^T \tag{100}$$

Similarly, we have the following expression

$$\boldsymbol{\Lambda}\, diag\left[r^{\kappa}\frac{\cos\pi\kappa}{1+2\kappa} \;\; r^{-\kappa}\frac{\cos\pi\kappa}{1-2\kappa} \;\; 1 \right] \boldsymbol{\Lambda}^{-1} = \mathbf{G}_1\zeta_1 + \mathbf{G}_2\zeta_2 + \mathbf{G}_3 \tag{101}$$

where

$$\zeta_1 = r^{\kappa}\frac{\cos\pi\kappa}{1+2\kappa}, \;\; \zeta_2 = r^{-\kappa}\frac{\cos\pi\kappa}{1-2\kappa} \tag{102}$$

$$\kappa = \frac{1}{2\pi i}\ln\frac{1-\beta}{1+\beta} = \frac{\tan^{-1}(-\beta)-\tan^{-1}\beta}{2\pi}, \;\; \beta = \sqrt{\frac{1}{2}tr[\mathbf{E}^2]} = \left[-\frac{a_5 f_{12} + a_6 f_{13}}{\nu_{11} a_1} \right]^{\frac{1}{2}} \tag{103}$$

$$\mathbf{G}_1 = \frac{1}{2\beta^2}\left[\mathbf{E}^2 + \beta\mathbf{E}\right], \;\; \mathbf{G}_2 = \frac{1}{2\beta^2}\left[\mathbf{E}^2 - \beta\mathbf{E}\right], \;\; \mathbf{G}_3 = \frac{-1}{\beta^2}\left[\mathbf{E}^2 - \beta^2\mathbf{I}\right] \tag{104}$$

Then, by means of Eqs. (94)-(96), we can express Eq. (100) as

$$\begin{aligned} [\delta_1 \;\; \delta_2 \;\; \delta_4]^T &= \frac{4\sqrt{r}}{\sqrt{2\pi}} \mathbf{H}\boldsymbol{\Lambda}\, diag\left[\zeta_1 \;\; \zeta_2 \;\; 1 \right] \boldsymbol{\Lambda}^{-1}\left(\mathbf{I}+\bar{\mathbf{H}}^{-1}\mathbf{H}\right)^{-1}[K_1 \; K_2 \; K_4]^T \\ &= \sqrt{\frac{2r}{\pi}}\left\{ \left[\frac{1}{2}(\zeta_1+\zeta_2) - 1 \right]\frac{1}{\beta^2}\mathbf{T}_3 + (\zeta_1-\zeta_2)\frac{1}{2\beta}\mathbf{T}_2 + \mathbf{T}_1 \right\}[K_1 \; K_2 \; K_4]^T \end{aligned} \tag{105}$$

or

$$\begin{aligned} \delta_1 &= \sqrt{\frac{2r}{\pi}}\left\{ \left[\frac{(\zeta_1+\zeta_2-2)(f_{12}a_5+f_{13}a_6)}{2\beta^2 a_1} + \nu_{11} \right] b_1 K_1 - (\zeta_1-\zeta_2)\frac{f_{12}b_1}{2\beta}K_2 + (\zeta_1-\zeta_2)\frac{f_{13}b_1}{2\beta}K_4 \right\} \\ \delta_2 &= \sqrt{\frac{2r}{\pi}}\left\{ (\zeta_1-\zeta_2)\frac{f_{12}b_1}{2\beta}K_1 + \left[\frac{a_2}{\nu_{11}} + (\zeta_1+\zeta_2-2)\frac{f_{12}^2 b_1}{2\beta^2\nu_{11}} \right] K_2 + \left[\frac{a_3}{\nu_{11}} + (\zeta_1+\zeta_2-2)\frac{f_{12}f_{13}b_1}{2\beta^2\nu_{11}} \right] K_4 \right\} \\ \delta_4 &= \sqrt{\frac{2r}{\pi}}\left\{ (\zeta_2-\zeta_1)\frac{f_{13}b_1}{2\beta}K_1 + \left[\frac{a_3}{\nu_{11}} + (\zeta_1+\zeta_2-2)\frac{f_{12}f_{13}b_1}{2\beta^2\nu_{11}} \right] K_2 + \left[\frac{a_4}{\nu_{11}} + (\zeta_1+\zeta_2-2)\frac{f_{13}^2 b_1}{2\beta^2\nu_{11}} \right] K_4 \right\}. \end{aligned} \tag{106}$$

Consequently, for both conditions 1 and 2 (sections 6.3.1 and 6.3.2), the relations between the

crack opening displacement and electric potential jump and the stress intensity factors can be written in a matrix form as

$$\begin{bmatrix} \delta_1 \\ \delta_2 \\ \delta_4 \end{bmatrix} = \sqrt{\frac{2r}{\pi}} \begin{bmatrix} d_{11} & d_{12} & -d_{13} \\ -d_{12} & d_{22} & d_{23} \\ d_{13} & d_{23} & d_{33} \end{bmatrix} \begin{bmatrix} K_1 \\ K_2 \\ K_4 \end{bmatrix} = \sqrt{\frac{2r}{\pi}}\mathbf{DK}, \tag{107}$$

where d_{ij} take the values in equation (99) for condition 1 and equation (106) for condition 2, respectively. Now, the dynamic J integral can be written as

$$J_1^0 = G = \frac{1}{4}\mathbf{K}^T\mathbf{U}\mathbf{K} = \frac{1}{4}\left[\nu_{11}b_1K_1^2 + a_2/\nu_{11}K_2^2 + a_4/\nu_{11}K_4^2 + 2a_3/\nu_{11}K_2K_4\right]. \tag{108}$$

We also denote $q_1=\delta_1/\delta_2$, $q_2=\delta_4/\delta_2$ and

$$n_1=b_{11}q_1-b_{12}+b_{13}q_2,\quad n_2=b_{12}q_1+b_{22}+b_{23}q_2,\quad n_4=-b_{13}q_1+b_{23}+b_{33}q_2, \tag{109}$$

where

$$b_{11}=d_{22}d_{33}-d_{23}^2,\ b_{12}=d_{13}d_{23}+d_{12}d_{33},\ b_{13}=d_{13}d_{22}+d_{12}d_{23},\ b_{22}=d_{11}d_{33}+d_{13}^2,\ b_{23}=d_{13}d_{12}-d_{11}d_{23},\ b_{33}=d_{11}d_{22}+d_{12}^2. \tag{110}$$

Then, combining Eqs. (107) and (108), we can obtain

$$K_j = 2n_j\mathbf{sgn}|\mathbf{D}|\sqrt{\frac{J_1^0}{\left|\nu_{11}b_1n_1^2+(a_2/\nu_{11})n_2^2+(a_4/\nu_{11})n_4^2+2(a_3/\nu_{11})n_2n_4\right|}},\ (j=1,2,4) \tag{111}$$

where

$$|\mathbf{D}| = d_{13}^2d_{22} + 2d_{12}d_{13}d_{23} - d_{23}^2d_{11} + d_{12}^2d_{33} + d_{11}d_{22}d_{33}. \tag{112}$$

The formulas in this section are applicable in both static and dynamic cases, and for stationary and propagating cracks. For a dynamically propagating crack, the matrix **H** depends on the crack velocity C.

The features of the component separation method can be summarized as follows:

(i) It can be expressed by explicit formulas.

(ii) It does not require any auxiliary solution field.

(iii) It is applicable using the path independent separated dynamic J integrals, the dynamic J integral, or the dynamic energy release rate.

7. Numerical examples

Consider a static interface crack of length 2a in an infinite bimaterial piezoelectric medium with crack fronts parallel to the X_3 axis as shown in Fig. 5. The primary loading is uniform remote tensile, shear and electric displacement loading $\mathbf{t}^0=[\sigma_{12}^\infty \sigma_{22}^\infty D_2^\infty]^T$. For condition 1, the analytical solution of stress and electric displacement intensity factors for this case was derived as (Shen and Kuang 1998):

$$[K_1\ K_2\ K_4]^T=\frac{\sqrt{\pi a}}{2}\left(\overline{\mathbf{H}}^{-1}+\mathbf{H}\right)\mathbf{H}\mathbf{\Lambda}diag\left[(1+2i\varepsilon)(2a)^{i\varepsilon}\quad(1-2i\varepsilon)(2a)^{i\varepsilon}\quad 1\right]\mathbf{\Lambda}^{-1}\left(\mathbf{I}+\overline{\mathbf{H}}^{-1}\mathbf{H}\right)^{-1}\mathbf{t}^0 \tag{113}$$

with

$$\mathbf{\Lambda}diag\left[(1+2i\varepsilon)\quad(1-2i\varepsilon)(2a)^{i\varepsilon}\quad 1\right]\mathbf{\Lambda}^{-1}=\mathbf{G}_1\xi_2+\overline{\mathbf{G}}_1\overline{\xi}_2+\mathbf{G}_3, \tag{114}$$

where

$$\xi_2=(1+2i\varepsilon)(2a)^{i\varepsilon}. \tag{115}$$

For condition 2, the analytical solution of stress and electric displacement intensity factors for this case was (Shen and Kuang 1998):

$$[K_1\ K_2\ K_4]^T=\frac{\sqrt{\pi a}}{2}\left(\overline{\mathbf{H}}^{-1}+\mathbf{H}^{-1}\right)\mathbf{H}\mathbf{\Lambda}diag\left[(1+2\kappa)(2a)^{\kappa}\quad(1-2\kappa)(2a)^{\kappa}\quad 1\right]\mathbf{\Lambda}^{-1}\left(\mathbf{I}+\overline{\mathbf{H}}^{-1}\mathbf{H}\right)^{-1}\mathbf{t}^0 \tag{116}$$

with

$$\mathbf{\Lambda}diag\left[(1+2\kappa)(2a)^{\kappa}\quad(1-2\kappa)(2a)^{\kappa}\quad 1\right]\mathbf{\Lambda}^{-1}=\mathbf{G}_1\xi_1+\mathbf{G}_2\xi_2+\mathbf{G}_3, \tag{117}$$

where

$$\xi_1=(1+2\kappa)(2a)^{\kappa},\ \xi_2=(1-2\kappa)(2a)^{\kappa}. \tag{118}$$

Then, for both conditions 1 and 2, by means of Eqs. (113)-(118), we can obtain

$$\begin{aligned}
K_1&=\sqrt{\pi a}\left(m_{11}\sigma_{12}^\infty+m_{12}\sigma_{22}^\infty+m_{13}D_2^\infty\right),\\
K_2&=\sqrt{\pi a}\left(m_{21}\sigma_{12}^\infty+m_{22}\sigma_{22}^\infty+m_{23}D_2^\infty\right),\\
K_4&=\sqrt{\pi a}\left(m_{31}\sigma_{12}^\infty+m_{32}\sigma_{22}^\infty+m_{33}D_2^\infty\right),
\end{aligned} \tag{119}$$

where

$$m_{11}=\frac{a_1}{b_0}g_{11},\ m_{12}=\frac{a_1}{b_0}g_{12},\ m_{13}=-\frac{a_1}{b_0}g_{13},$$

$$m_{21}=\frac{a_4g_{12}+a_3g_{13}}{b_0},\ m_{22}=\frac{a_3g_{23}-a_4g_{22}}{b_0},\ m_{23}=\frac{a_3g_{33}-a_4g_{23}}{b_0},$$

$$m_{31}=\frac{-a_3g_{12}-a_2g_{13}}{b_0},\ m_{32}=\frac{a_3g_{22}-a_2g_{23}}{b_0},\ m_{33}=\frac{a_3g_{23}-a_2g_{33}}{b_0}, \tag{120}$$

with

$$g_{11}=\left[\left(1-\mathbf{Re}\,\xi_2\right)\frac{f_{12}a_5+f_{13}a_6}{\beta^2a_1}+\nu_{11}\right]b_1,\ g_{12}=\mathbf{Im}\,\xi_2\frac{f_{12}b_1}{\beta}$$

$$g_{13}=\mathbf{Im}\,\xi_2\frac{f_{13}b_1}{\beta},\ g_{22}=\frac{a_2}{\nu_{11}}\left(1-\mathbf{Re}\,\xi_2\right)\frac{f_{12}^2b_1}{\beta^2\nu_{11}}$$

$$g_{23}=\frac{a_3}{\nu_{11}}+\left(1-\mathbf{Re}\,\xi_2\right)\frac{f_{12}f_{13}b_1}{\beta^2\nu_{11}},\ g_{33}=\frac{a_4}{\nu_{11}}\left(1-\mathbf{Re}\,\xi_2\right)\frac{f_{13}^2b_1}{\beta^2\nu_{11}} \tag{121}$$

for condition 1, and

$$g_{11}=\left[\left(\xi_1+\xi_2-2\right)\frac{f_{12}a_5+f_{13}a_6}{2\beta^2a_1}+\nu_{11}\right]b_1,\ g_{12}=\left(\xi_2-\xi_1\right)\frac{f_{12}b_1}{2\beta}$$

$$g_{13}=\left(\xi_2-\xi_1\right)\frac{f_{13}b_1}{2\beta},\ g_{22}=\frac{a_2}{\nu_{11}}\left(\xi_1+\xi_2-2\right)\frac{f_{12}^2b_1}{2\beta^2\nu_{11}}$$

$$g_{23}=\frac{a_3}{\nu_{11}}+\left(\xi_1+\xi_2-2\right)\frac{f_{12}f_{13}b_1}{2\beta^2\nu_{11}},\ g_{33}=\frac{a_4}{\nu_{11}}\left(\xi_1+\xi_2-2\right)\frac{f_{13}^2b_1}{2\beta^2\nu_{11}} \tag{122}$$

for condition 2.

In the following numerical study, a bimaterial system composed of PZT-4 and PZT-5H with a stationary center crack subjected to static uniform remote tension σ_{22}^{∞}=1MPa and electric displacement D_2^{∞}=0.001C/m^2 is considered. The specimen dimensions of 40×40mm with the center crack of 2a=4mm, and loading conditions are shown in Fig. 5. The finite element method (Shen and Nishioka 2002) is used to analyze the problem. The finite element mesh, representing the right half of the structure, is shown in Fig. 6, enclosing the near-tip details and the far-field paths to be used for calculating the separated generalized (dynamic) J integral. Eight-node isoparametric elements were used in the analysis.

The material parameters for PZT-4 are given below:

Elastic Constants (GPa)

c_{11}=139.0, c_{12}=77.8, c_{13}=74.3, c_{33}=113.0, c_{44}=25.6;

Piezoelectric constants (C/m^2):

e_{31}=-6.98, e_{33}=13.84, e_{15}=13.44;

Dielectric constants (nF/m):

κ_{11}=6.00, κ_{33}=6.00;

and those for PZT-5H are:

Elastic Constants (GPa)

c_{11}=126.0, c_{12}=55.0, c_{13}=53.0, c_{33}=117.0, c_{44}=35.3;

Piezoelectric constants (C/m^2):

e_{31}=-6.5, e_{33}=23.3, e_{15}=17.0;

Dielectric constants (nF/m):

κ_{11}=15.1, κ_{33}=13.0;

where C and F denote Coulomb and Farad, respectively. Strong piezoelectric coupling effects can be expected as $|e_{33}/(\kappa_{33}c_{33})^{0.5}|$=0.5567 for PZT-4, and $|e_{33}/(\kappa_{33}c_{33})^{0.5}|$=0.5974 for PZT-5H (lower piezoelectric coupling is present for $|e_{33}/(\kappa_{33}c_{33})^{0.5}|$<<1). In this example, the oscillatory singularity is real, i.e. tr[$\mathbf{E}^2$]>0.

In this finite-element analysis, first, the separated generalized J integrals are evaluated by Eq. (67) for five circular far-field integral paths (see Fig. 6(b)). Figure 7 indicates excellent path independence of the separated generalized J integrals for the interfacial crack subject to combined eletromechanical loading. The generalized J integral values are obtained by the sum of the separated ones (see Eq. (70)), and these are converted to the stress and electric displacement intensity factors using the component separation method (see Eq. (111)).

Note that the dimensions of the medium are finite. Thus, the stress and electric displacement intensity factors should be influenced by the finite boundaries. In this case, the stress and electric displacement intensity factors can be expressed by

$$K_j = F_j\, K_j^{\infty},\ (j=1,2,4), \tag{123}$$

where F_j $(j=1,2,4)$ are finite correction factors for this problem. However, in literature the correction factors for piezoelectric interface cracks are not available. Thus we assume that those are nearly the same as the finite correction factor of the central crack in square elastic homogeneous plate under tension (Isida 1971). Then the stress and electric displacement intensity factors for the finite piezoelectric bimaterial plate are inferred as

$$K_j^{Semi\text{-}Anal} \approx F_1 K_j^{\infty Anal}, \tag{124}$$

where $F_1=1.014$ for $a/d=0.1$, and $K_j^{\infty Anal}$ $(j=1,2,4)$ are the analytical solutions of stress and electric displacement intensity factors in an infinite plate $(a/d=0)$ given by Eq. (119) (Shen and Kuang 1998). Thus, $K_j^{Semi\text{-}Anal}$ $(j=1,2,4)$ are considered as the semi-analytical solutions for this problem.

The simulated stress and electric displacement intensity factors with the semi-analytical solution given by Eq. (124) are presented in Tables 1 to 3 for mechanical, electrical and combined loading, respectively. In these tables, two types of errors are used. One is the relative error to the corresponding semi-analytical solution:

$$\varepsilon_j^r = \left(K_j^{FEM} - K_j^{Semi\text{-}Anal}\right) / K_j^{Semi\text{-}Anal}, \ (j=1,2,4). \tag{125}$$

However, the relative error is not a good measure when one of the corresponding exact solutions is zero or close to zero. The other is the error compared with the solution norm:

$$\varepsilon_j^n = \left(K_j^{FEM} - K_j^{Semi\text{-}Anal}\right) / \sqrt{\left(K_1^{Semi\text{-}Anal}\right)^2 + \left(K_2^{Semi\text{-}Anal}\right)^2 + \left(K_4^{Semi\text{-}Anal}\right)^2}, \ (j=1,2,4), \tag{126}$$

where $\sqrt{\left(K_1^{Semi\text{-}Anal}\right)^2 + \left(K_2^{Semi\text{-}Anal}\right)^2 + \left(K_4^{Semi\text{-}Anal}\right)^2}$ is the norm in the solution space of (K_1, K_2, K_4). Although the dimension of K_4 differs from the others, the solution norm can be still used as a measure of the magnitude of the intensities.

The crack opening displacements and electric potential jumps are taken from the third to sixth elements behind the crack tip. The results are almost independent from the distance r. Thus, extrapolation to the crack tip is not necessary when the component separation method is used. It is shown that the errors ε_j^n of the dominant intensity factors (K_2 in Table 1, K_4 in Table 2, K_2 and K_4 in Table 3) are within 0.7%. For non-dominant intensities K_1 and K_4 under tension (see Table 1), K_1

and K_2 under electric loading (see Table 2), and K_I under combined loading, the errors ε_j^n are within 1.2%. Therefore, it can be concluded that the accuracy of the component separation method of the path independent generalized J integral is extremely good.

It is also interesting to note that, when only the electric loading is applied (see Table 2), the searing (mode II) deformation couples with electric field more strongly than the tensile (mode I) deformation does.

8. Conclusions

In this paper, first, the near-tip stress and electric displacement fields were analytically solved for a dynamically propagating crack in a piezoelectric bimaterial. Especially, the explicit expression of the crack opening displacements and electric potential jump in terms of the stress and electric displacement intensity factors were also derived.

Second, from the rate formulation of the energy balance in a piezoelectric material, the near-field expressions of the dynamic J integral and dynamic energy release rate were derived. Furthermore, based on the near-field expression of the dynamic J integral, the path independent dynamic J integral was derived for arbitrary far-field paths. The equivalent domain integral expression of the dynamic J integral was also obtained. Using the near-tip analytical solutions presently obtained, the relationships between the dynamic J integral and the stress and electric displacement intensity factors were also obtained. It was shown that the path independent dynamic J integral contains the static J integral (Rice 1968) and the dynamic J integral (Nishioka and Atluri 1983) for elastic materials, and static J integral (Cherepanov 1979, Pak 1990, Kuna 1998) for piezoelectric materials as special cases.

Third, the concept of the separated dynamic J integral (Nishioka and Yasin 1999) was extended to an interfacial crack in a piezoelectric bimaterial. The separated dynamic J integrals for an interfacial crack have the physical significance of energy flow rates into the propagating interfacial crack tip from the individual material sides or, equivalently, the separated dynamic

energy release rates.

Fourth, to accurately evaluate mixed-mode stress and electric displacement intensity factors, the component separation method of the dynamic J integral was developed. This method has more advantage over the M_1 integral method that is commonly used for interfacial crack problems.

Finally, the finite element analyses of a static stationary interfacial crack in the piezoelectric bimaterial of PZT-4 and PZT-5H subject to mechanical, electrical and combined loadings were carried out. The path independence of the generalized (dynamic) J integral as well as the separated J integral was verified from the numerical results. The generalized J integral values were utilized to calculate the stress and electric displacement intensity factors based on the component separation method. The intensity factors calculated were extremely accurate, and almost independent from the evaluation points. Thus, no extrapolation to the crack tip is necessary when the component separation method is used.

Acknowledgements: This study was supported by the Grant-in-Aid for Scientific Research (No.14205019) from the Ministry of Education, Science and Culture in Japan, and also by the natural science grant from Mitsubishi Foundation.

References

S.N. Atluri, T. Nishioka and M. Nakagaki, Incremental path-independent integrals in inelastic and dynamic fracture mechanics. *Engineering Fracture Mechanics* **20-2** (1984), pp.209-244.

H.G. Beom and S.N. Atluri, Near-tip fields and intensity factors for interfacial cracks in dissimilar anisotropic piezoelectric media. *International Journal of Fracture* **75** (1996) pp.163-183.

B. Budiansky and J.R. Rice, Conservation laws and energy release rates. *Journal of Applied Mechanics* **40** (1973) pp.201-203.

G.P. Cherepanov, *Mechanics of Brittle Fracture*, McGraw-Hill, New York (1979).

C. Dascalu and G.A. Maugin, Dynamic fracture for piezoelectric material. *The Quarterly Journal of Mechanics and Applied Mathematics* **48** (1995) pp.237.

L.B. Freund, Energy flux into the tip of an extending crack in an elastic solid. *Journal of Elasticity* **2** (1972) pp.341-349.

C. Hwu, Fracture parameters for the orthotropic bimaterial interface cracks. *Engineering Fracture Mechanics* **45** (1993) pp.89-97.

M. Isida, Effect of width and length on stress intensity factors of internally cracked plates under various boundary conditions, *International Journal of Fracture Mechanics* **7** (1971) pp.301-316.

M. Kuna, Finite element analyses of crack problems in piezoelectric structures. *Computational Materials Science* **17** (1998) pp.67-80.

C.M. Kuo and D.M. Barnett, Stress singularities of interfacial cracks in bonded piezoelectric half-spaces. In J.J. Wu, T.C.T. Ting and D.M. Barnett (eds.) *Modern Theory of Anisotropic Elasticity and Applications*. SIAM, (1991) 33.

B. Moran and C.F. Shih, Crack tip and associated domain integrals from momentum and energy balance. *Engineering Fracture Mechanics* **27** (1987) pp.615-642.

G.P. Nikishkov and S.N. Atluri, Calculation of fracture mechanics parameters for an arbitrary three-dimensional crack, by the equivalent domain integral. *International Journal for Numerical Methods in Engineering* **24** (1987) pp.1801-1821.

T. Nishioka and S.N. Atluri, Path-independent integrals, energy release rates and general solutions of near-tip fields in mixed-mode dynamic fracture mechanics. *Engineering Fracture Mechanics* **18** (1983) pp.1-22.

T. Nishioka, R. Murakami and Y. Takemoto, The use of the dynamic *J* integral (J') in finite element simulation of mode I and mixed-mode dynamic crack propagation. *International Journal of Pressure Vessels and Piping* **44** (1990) pp.329-352.

T. Nishioka, Y. Ichikawa and N. Maeda, Numerical study on three-dimensional dynamic fracture. In T. Nishioka and J.S. Epstein (eds.) *Dynamic Fracture, Failure and Deformation.* The American Society of Mechanical Engineers, ASME Publication PVP-Vol.300 (1995) pp.73-85.

T. Nishioka and A. Yasin, The dynamic J integral, separated dynamic J integrals and moving finite element simulations for subsonic, transonic and supersonic interfacial crack propagation. *JSME International Journal*, Series A **42** (1999) pp.25-39.

T. Nishioka, S. Syano and T. Fujimoto, Concepts of separated J integrals, separated energy release rates and the component separation method of the J integral for interfacial fracture mechanics. *Journal of Applied Mechanics* (2003) (in press).

T. Nishioka and S. Shen, Higher order asymptotic solution for an interfacial crack in piezoelectric bimaterial under impact. *Materials Science Research International* **7-3** (2001) pp.157-165.

T. Nishioka, Q. Hu and T. Fujimoto, Component separation method of the dynamic J integral for evaluating mixed-mode stress intensity factors in dynamic interfacial fracture mechanics problems. *JSME International Journal,* Series A **45** (2002) pp.395-406.

T. Nishioka, J.H. Yu and S.P. Shen, Mechanical and electrical dynamic J integrals and energy release rates for interfacial dynamic crack in piezoelectric material. (2002) (submitted).

Y.E. Pak, Crack extension force in a piezoelectric material. *Journal of Applied Mechanics* **57** (1990) pp.647-653.

J.R. Rice, A path independent integral and approximate analysis of strain concentration by notches and cracks. *Journal of Applied Mechanics* **35** (1968) pp.379-386.

Z. Suo, C.M. Kuo and D.M. Barnett and J.R. Willis, Fracture mechanics for piezoelectric ceramics. *Journal of the Mechanics and Physics of Solids* **40** (1992) pp.739-765.

S. Shen and Z.B. Kuang, Interface crack in bi-piezothermoelastic media and the interaction with a point heat source. *International Journal of Solids and Structures* **35** (1998) pp.3899-3915.

S.P. Shen and T. Nishioka, Finite element analysis of impact interfacial crack problems in piezoelectric bimaterials. (2002) (submitted).

H.F. Tiersten, *Linear Piezoelectric Plate Vibrations.* Plenum Press, New York (1969).

J.F. Yau and S.S. Wang, An analysis of interface cracks between dissimilar isotropic materials using conservation integrals in elasticity. *Engineering Fracture Mechanics* **20- 3** (1984) pp.423-432.

K.C. Wu, Explicit crack-tip fields of an extending interface crack in an anisotropic bimaterial. *International Journal of Solids and Structures* **27** (1991) pp.455-466.

Table 1 Comparison of FEM-results with the semi-analytical solutions for the electromechanical interfacial crack subjected to tension

Element No.	r/a	K_1 ($MPam^{-1/2}$)			K_2 ($MPam^{-1/2}$)			K_4 ($10^{-3}Cm^{-3/2}$)		
		FEM present	Error (%)		FEM present	Error (%)		FEM present	Error (%)	
			ε^r_1	ε^n_1		ε^r_2	ε^n_2		ε^r_4	ε^n_4
Third	0.125	1.868×10^{-3}	3.54	0.08	8.013×10^{-2}	-0.45	-0.45	-1.630×10^{-4}	-29.4	-0.05
Fourth	0.175	1.855×10^{-3}	2.82	0.06	8.011×10^{-2}	-0.47	-0.47	-1.431×10^{-4}	-13.6	-0.02
Fifth	0.250	1.846×10^{-3}	2.32	0.05	8.009×10^{-2}	-0.50	-0.50	-1.272×10^{-4}	-2.35	-0.00
Sixth	0.325	1.845×10^{-3}	2.27	0.05	8.008×10^{-2}	-0.51	-0.51	-1.190×10^{-4}	-0.95	0.01
Semi-Analytical		1.804×10^{-3}			8.049×10^{-2}			-1.260×10^{-4}		

Table 2 Comparison of FEM-results with the semi-analytical solutions for the electromechanical interfacial crack subjected to electric displacement

Element No.	r/a	K_1 ($MPam^{-1/2}$)			K_2 ($MPam^{-1/2}$)			K_4 ($10^{-3}Cm^{-3/2}$)		
		FEM present	Error (%)		FEM present	Error (%)		FEM present	Error (%)	
			ε^r_1	ε^n_1		ε^r_2	ε^n_2		ε^r_4	ε^n_4
Third	0.125	-5.770×10^{-2}	0.10	0.10	-3.336×10^{-3}	6.87	0.43	8.339×10^{-2}	-1.22	-0.16
Fourth	0.175	-5.784×10^{-2}	-0.14	-0.14	-3.430×10^{-3}	4.24	0.26	8.339×10^{-2}	-1.22	-0.16
Fifth	0.250	-5.812×10^{-2}	-0.62	-0.62	-3.525×10^{-3}	1.59	0.10	8.342×10^{-2}	-1.18	-0.14
Sixth	0.325	-5.843×10^{-2}	-1.16	-1.16	-3.597×10^{-3}	-0.42	-0.02	8.346×10^{-2}	-1.14	-0.11
Semi-Analytical		-5.776×10^{-2}			-3.582×10^{-3}			8.442×10^{-2}		

Table 3 Comparison of FEM-results the semi-analytical solutions for the electromechanical interfacial crack subjected to combined loading

Element No.	r/a	K_1 ($MPam^{-1/2}$)			K_2 ($MPam^{-1/2}$)			K_4 ($10^{-3}Cm^{-3/2}$)		
		FEM present	Error (%)		FEM present	Error (%)		FEM present	Error (%)	
			ε^r_1	ε^n_1		ε^r_2	ε^n_2		ε^r_4	ε^n_4
Third	0.125	-5.640×10^{-2}	-0.84	-0.49	7.700×10^{-2}	0.13	0.11	8.406×10^{-2}	-0.26	-0.23
Fourth	0.175	-5.645×10^{-2}	-0.93	-0.55	7.678×10^{-2}	-0.16	-0.13	8.393×10^{-2}	-0.42	-0.37
Fifth	0.250	-5.662×10^{-2}	-1.23	-0.73	7.651×10^{-2}	-0.51	-0.42	8.380×10^{-2}	-0.57	-0.51
Sixth	0.325	-5.689×10^{-2}	-1.72	-1.00	7.625×10^{-2}	-0.85	-0.69	8.377×10^{-2}	-0.61	-0.54
Semi-Analytical		-5.593×10^{-2}			7.690×10^{-2}			8.428×10^{-2}		

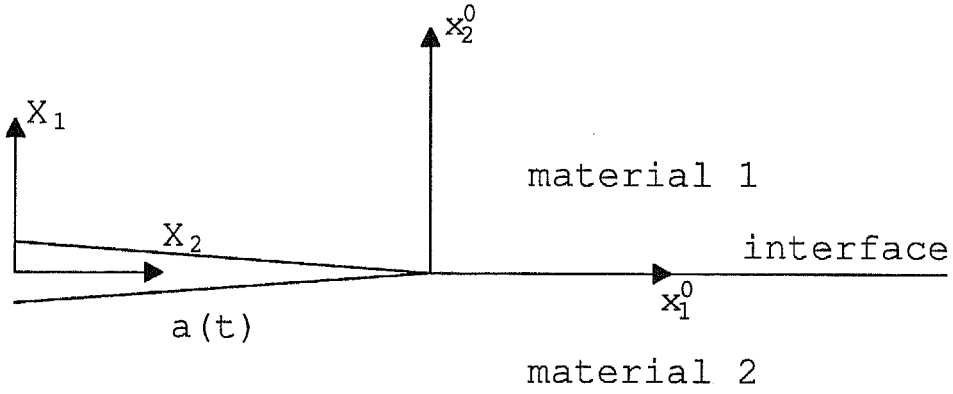


Figure 1 An interface crack in a semi-infinite piezoelectric bimatrials

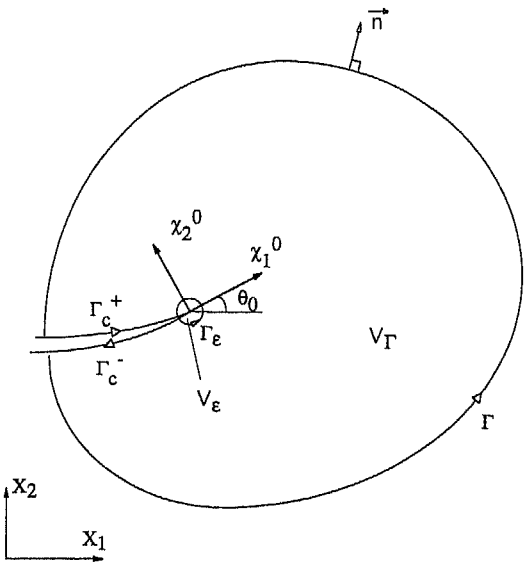


Figure 2 Crack in homogeneous material

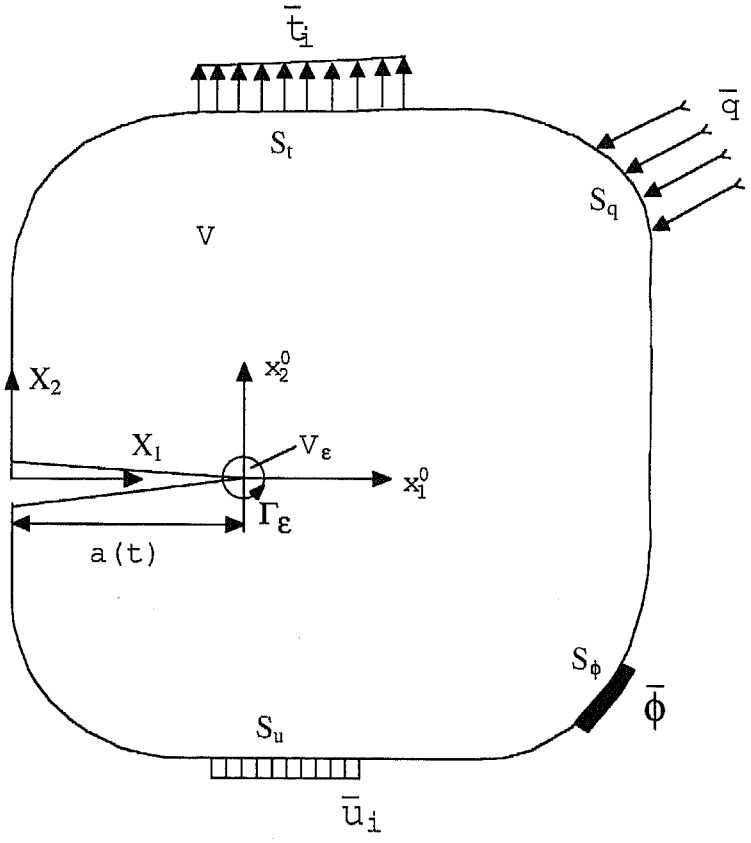


Figure 3 Dynamically propagating crack in a piezoelectric material

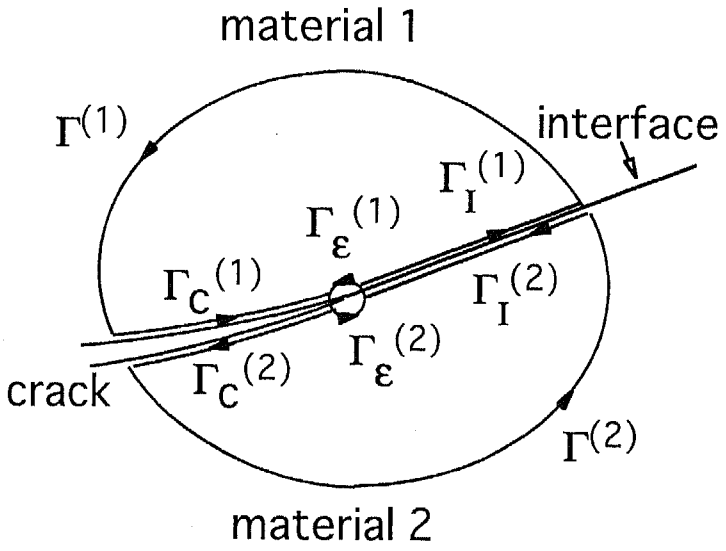


Figure 4 Interfacial crack in a nonhomogeneous piezoelectric material

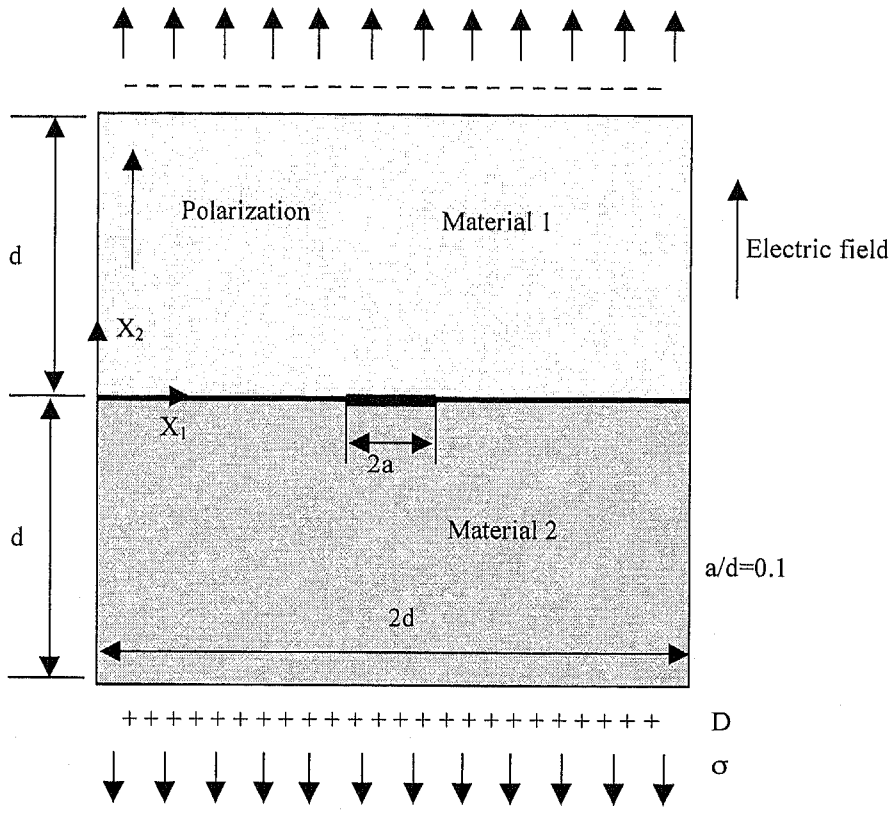
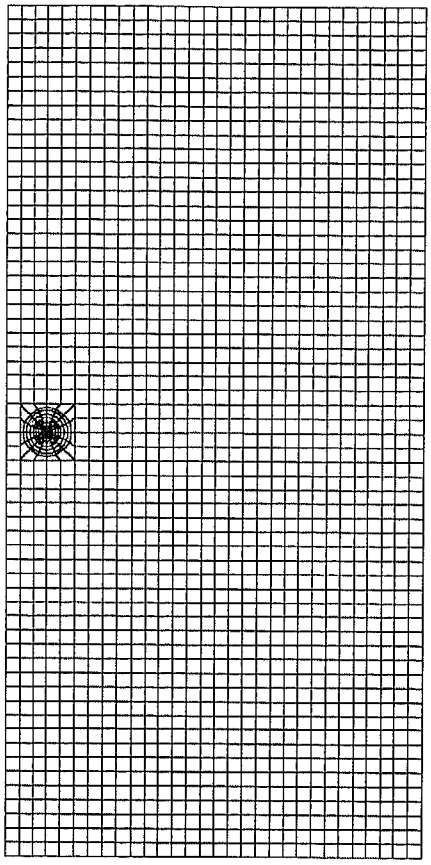
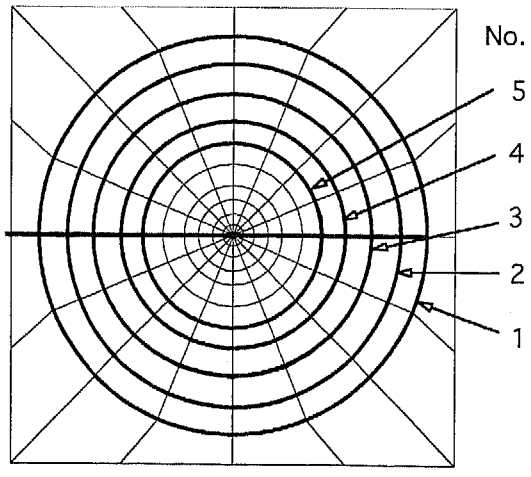


Figure 5 Interfacial center crack in a piezoelectric bimaterial



(a) Mesh pattern (1/2 of the structure, 1960 elements, 6069 nodes)



(b) Crack tip elements and the integral paths

Figure 6 Mesh pattern and integral paths

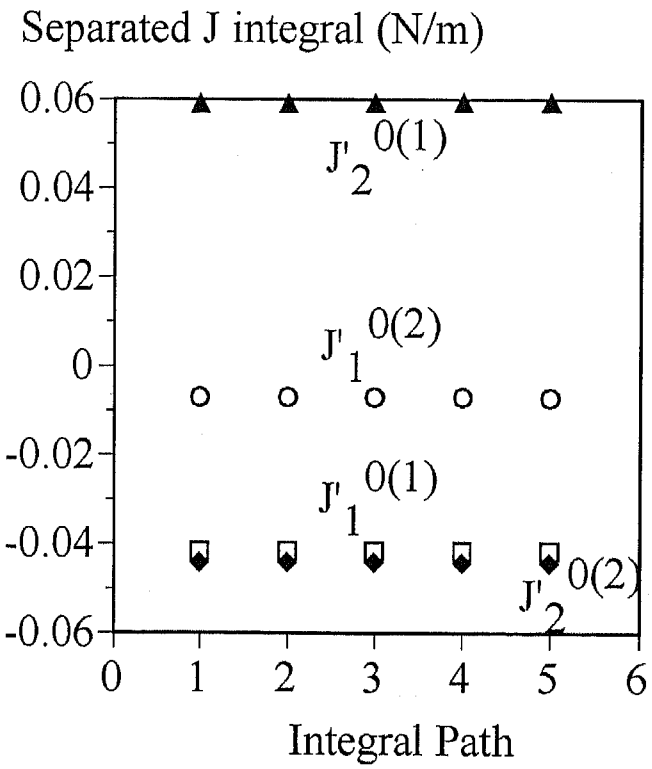


Figure 7 Path independence of separated generalized J integrals in piezoelectric bimaterial